



Defence Research and  
Development Canada

Recherche et développement  
pour la défense Canada



# Shear Lip/Plastic Zone Finite Element Model Development

*B.K. Gallant  
T.S. Koko*

*Martec Limited  
400-1888 Brunswick Street  
Halifax, Nova Scotia  
B3J 3J8*

*Contract Number: W7707-8-6180/A*

*Contract Scientific Authority: J.R. Matthews, (902) 427-0550 x3444*

**Defence R&D Canada**

Contract Report

DRDC Atlantic CR 2002-178

October 2002

**Canada**

# **Shear Lip/Plastic Zone Finite Element Model Development**

B.K. Gallant  
T.S. Koko

Martec Limited  
400-1888 Brunswick Street  
Halifax, Nova Scotia  
B3J 3J8

Contract number: W7707-8-6180/A

Contract Scientific Authority: J.R. Matthews, (902) 427-0550 x 3444

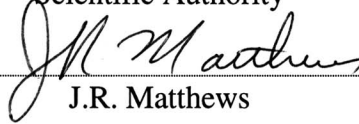
**Defence R&D Canada – Atlantic**

**Contract Report**

DRDC Atlantic CR 2002-178

October 2002

Scientific Authority



---

J.R. Matthews

Approved by

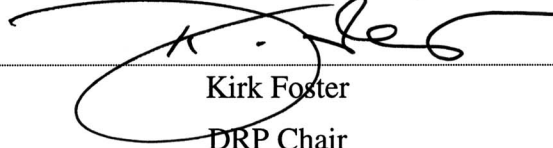


---

R.M. Morchat

H/EMat

Approved for release by



---

Kirk Foster

DRP Chair

The scientific or technical validity of this Contract Report is entirely the responsibility of the contractor and the contents do not necessarily have the approval or endorsement of Defence R&D Canada

## Abstract

---

This study focused on the development of shear-lip in DT specimens under quasi-static loading rate. The objective of the study was to demonstrate the feasibility of a numerical simulation of shear-lips for a 25mm base metal DT specimen in three-point bend test. Three real stress-real strain curves representing three different materials with varying degrees of plastic behaviour were considered. These material curves are designated as Curves 1, 2 and 3. Curve 1 represents the actual real-stress- real-strain curve of the 350WT steel material. On the other hand, Curve 2 represents the same curve, but with the fracture strain reduced to half that of Curve 1; while Curve 3 represents a similar curve as Curve 1, but with the yield stress reduced to half the Curve 1 value.

Crack advance and element or node release was based on two possible criteria, namely (a) when the average strain in the crack tip elements that occupy a physical surface of 1.25 mm (0.050 inches) exceeds the strain at fracture on the supplied data; and (b) when the strain energy density in elements occupying a volume defined by 1.25 mm (0.050 inches) of free surface at the crack tip and 1.25 mm (0.050 inches) of material depth exceeds the strain energy density calculated from the supplied real stress real strain curves.

It was shown that the plastic strain contour patterns obtained from the finite element analyses could be used to estimate the shear-lip sizes. At any given crack size ( $a/W$  level), the shear-lip size is smallest for Curve 2 material and largest for Curve 3. This trend is reasonable as the Curve 2 material is the least plastic (100% strain to failure as opposed to 200% strain for Curves 1 and 3); and the Curve 3 material is the most plastic (has lower yield stress of 197MPa compared to 395MPa for Curves 1 and 2, and high failure strain of 200%). For a given material, the shear-lip size tends to reduce with increasing crack size. For instance, for the Curve 1 material, the shear-lip sizes for  $a/W = 0.4, 0.45$  and  $0.5$  are 10.95mm, 10.30mm and 9.70mm, respectively. The same trends of shear-lip sizes were observed, regardless of whether the plastic strain criterion or strain energy density criterion was used for crack advance. However, for any given material and crack size, the shear-lip size predicted based on the strain energy density criterion was greater than that predicted based on the plastic strain criterion.

## Résumé

---

Les principaux travaux de la présente étude portaient sur la croissance du débord de rupture dans des éprouvettes de torsion ductile, pour une vitesse de mise en charge quasi statique. Ils visaient à démontrer l'applicabilité de la modélisation numérique des débords de rupture dans le cas d'une éprouvette de torsion ductile en métal, de 25 mm, soumise à un essai de pliage en trois points. On a examiné les cas des courbes effort réel-déformation réelle, appelées Courbes 1, 2 et 3, représentant trois matériaux caractérisés par des comportements plastiques distincts. La Courbe 1 représente la courbe effort réel-déformation réelle expérimentale obtenue pour l'acier 350WT. La Courbe 2, quant à elle, correspond au même type de courbe, avec, toutefois, une valeur réduite de déformation à la rupture, afin d'obtenir une valeur équivalente à celle de la Courbe 1. Dans le cas de la Courbe 3, qui est semblable à la Courbe 1, c'est la limite apparente d'élasticité qui a été réduite de moitié par rapport à celle de la Courbe 1. La propagation de la fissure et la relâche de la contrainte appliquée aux éléments ou aux nœuds étaient basées sur deux critères possibles : a) lorsque la déformation moyenne, dans les éléments de l'extrémité de fissure qui occupent une dimension matérielle de 1,25 mm (0,050 po), est supérieure à la déformation à la rupture, selon les données fournies, et b) lorsque la densité d'énergie de déformation, dans des éléments occupant un volume délimité par une dimension libre de 1,25 mm (0,050 po) à l'extrémité de fissure et par une profondeur de 1,25 mm (0,050 po), est supérieure à la valeur de la densité d'énergie de déformation calculée à partir des courbes effort réel-déformation réelle fournies.

Il a été démontré que les courbes modèles de déformation plastique obtenues grâce à l'analyse par éléments finis peuvent servir à estimer la taille des débords de rupture. Pour toute taille de la fissure (niveau de  $a/W$ ), la taille du débord de rupture est minimale dans le cas du matériau de la Courbe 2 et maximale dans le cas de celui de la Courbe 3. Cette observation est acceptable, car le matériau de la Courbe 2 est le moins plastique des trois (100 % de déformation à la rupture, par rapport à 200 % de déformation à la rupture, dans le cas des Courbes 1 et 3), et le matériau de la Courbe 3 est le plus plastique (il est caractérisé par une faible limite apparente d'élasticité de 197 MPa, comparativement à 395 MPa, pour les Courbes 1 et 2, et par une déformation à la rupture élevée, soit 200 %). Pour un matériau donné, la taille du débord de rupture tend à diminuer en fonction de l'accroissement de la taille de la fissure. Ainsi, dans le cas du matériau de la Courbe 1, la taille des débords de rupture est respectivement de 10,95 mm, 10,30 mm et 9,70 mm, pour des valeurs de  $a/W$  de 0,4, 0,45 et 0,5. Ces tendances relatives à la variation de la taille des débords de rupture ont été observées dans le cas des deux critères susmentionnés de propagation de la fissure, soit celui de la déformation plastique et celui de la densité d'énergie de déformation. Toutefois, pour tout matériau donné et toute taille donnée de la fissure, la valeur prévue de la taille du débord de fissure basée sur le critère de la densité d'énergie de déformation était toujours supérieure à celle prévue pour le critère de la déformation plastique.

# **Executive summary**

---

## **Introduction or Background**

Over the past two decades, Defence R&D Canada has conducted research in fracture mechanics and fracture control and has identified shear lip as the most economical and practical material property for assessing fracture toughness and location in the transition curve for steel and weldments.

In 1991 DRDC Atlantic first published their theory that the plastic zone at initiation of crack advance and the developing shear lip were approximately equal. Over the past ten years DRDC has tried to verify this experimentally and in the past two years has supported work in several locations to try to verify this numerically with finite element models.

This contract was Martec's first attempt to determine the plastic zone shear lip relationship.

## **Results**

Martec's model was not fine enough to provide a definitive plastic zone size at crack initiation. However, comparison with their work on shear lip and stretch zone showed that the plastic zone size obtained for the 25 mm specimen was about 9 mm at  $DL/B=0.03$ ; whereas, from the present study, the shear lip size is 9.7-10.95 mm. If it can be established that crack initiation starts around  $DL/B=0.03$ , then their analysis supports the DRDC hypothesis.

## **Significance**

This is a major element of fracture control theory and its verification by FE greatly simplifies the approach to determining risk of fracture in naval vessels.

## **Future Plans**

To help this approach gain wide acceptance DRDC hopes to refine the approach to shear lip determination in additional configurations. Accordingly further FE model work is planned.

**Gallant, B.K. and Koko, T.S., 2002, Shear Lip/ Plastic Zone Finite Element Model Development, CR 2002-178, Defence R&D Canada - Atlantic.**

# Sommaire

---

## Introduction ou historique

Au cours des deux dernières décennies, R & D pour la défense Canada (RDDC) a effectué des travaux de recherche dans les domaines de la mécanique de la rupture et sa prévention. Les résultats ont permis d'établir que pour évaluer la résistance à la rupture (ou ténacité) et la position de la fracture dans la courbe de transition de l'acier et des assemblages soudés, le débord de rupture constitue la caractéristique matérielle dont l'analyse est la plus économique et pratique.

En 1991, RDDC Atlantique publiait sa théorie selon laquelle la taille de la zone plastique à l'amorçage de la propagation de la fissure et celle du débord de rupture en développement étaient approximativement égales. Depuis dix ans, RDDC tente d'apporter une confirmation expérimentale à la théorie et, au cours des deux dernières années, elle a soutenu les travaux de différents centres de recherche visant la validation numérique de la théorie à partir de modèles d'éléments finis.

Le présent contrat constituait les premiers travaux de la société Martec visant à déterminer la relation entre la zone plastique et le débord de rupture.

## Résultats

Le modèle utilisé par la société Martec n'était pas assez raffiné pour permettre de bien déterminer la taille de la zone plastique à l'amorçage de la fissure. Toutefois, en comparant les résultats avec ceux obtenus lors de leurs travaux portant sur le débord de rupture et la zone d'étirement, on a établi que la taille de la zone plastique était d'environ 9 mm, dans le cas de l'échantillon de 25 mm, pour un rapport  $DL/B = 0,03$ . Cependant, dans la présente étude, la taille du débord de rupture se situe entre 9,7 et 10,95 mm. Si les résultats démontrent que l'amorçage de la fissure correspond à une valeur approximative de  $DL/B = 0,03$ , l'analyse soutient l'hypothèse de la RDDC.

## Importance des résultats

Il s'agit d'un élément majeur de la théorie de la prévention des ruptures. Sa vérification par l'analyse par éléments finis simplifiera grandement les méthodes de détermination des risques de rupture dans les navires de guerre.

## Futurs travaux

Pour que cette méthode soit largement acceptée, RDDC souhaite la raffiner et l'utiliser pour déterminer les débords de rupture dans des configurations supplémentaires. Par conséquent, on prévoit exécuter d'autres travaux de modélisation par éléments finis.

**Gallant, B.K. et Koko, T.S., 2002, Shear Lip/ Plastic Zone Finite Element Model Development, CR 2002-178, R & D pour la défense Canada - Atlantique.**

# Table of contents

---

Abstract.....	i
Executive summary.....	iii
Sommaire.....	iv
Table of contents.....	v
List of figures.....	vi
Acknowledgements.....	viii
1. INTRODUCTION.....	1
1.1 Background .....	1
1.2 Objectives and Scope .....	1
2. PROBLEM DESCRIPTION .....	2
2.1 Specimen Configurations .....	2
2.2 Description of Shear-Lip and Plastic Zone in DT Specimens .....	2
2.3 Requirements.....	2
3. FINITE ELEMENT MODEL .....	7
3.1 Finite Element Approach .....	7
3.1.1 Element Removal Process in ABAQUS .....	7
3.2 Finite Element Meshes.....	8
3.3 Material Models .....	8
3.4 Boundary Conditions and Loading .....	9
4. RESULTS AND DISCUSSIONS .....	13
4.1 Strain Energy Densities for the Three Curves.....	13
4.2 Shear-Lip and Plastic Zone Development with Maximum Strain Criteria .....	13
4.3 Shear-Lip Development with Strain Energy Density Criteria .....	15
5. SUMMARY, CONCLUSIONS AND RECOMMENDATIONS .....	32
5.1 Summary and Conclusions.....	32
5.2 Recommendations .....	33
6. REFERENCES.....	34



## List of figures

---

Figure 2.1: Configuration of DT Specimen .....	4
Figure 2.2: Graphical Representation of Material Test Data to be Used in Analyses .....	5
Figure 2.3: Schematic of DT Specimen Showing Plastic Zone .....	5
Figure 2.4: Schematic of Cross-Section of DT Specimens Showing Shear-Lip Formation .....	6
Figure 3.1: Flow Chart Showing the Procedure Used for Element Removal in ABAQUS Environment .....	10
Figure 3.2: Finite Element Mesh of Standard DT Specimen .....	11
Figure 3.3: Finite Element Model of Standard DT Specimen Showing Applied Loading and Boundary Conditions .....	12
Figure 4.1: Plastic Strain Contours at $D_L = 6.29\text{mm}$ .....	16
Figure 4.2: Finite Element Mesh Showing Elements For Which Results are Stored .....	17
Figure 4.3: Schematic of Crack Face Showing Method of Determining Shear-Lip Size .....	17
Figure 4.4: (a) Plastic Strain Contours, (b) Crack Propagation and (c) Close-up View of Plastic Strain Contours for Model With Curve 1 Material Properties Using Plastic Strain as Removal Criterion ( $a/W = 0.4$ ) .....	18
Figure 4.5: (a) Plastic Strain Contours, (b) Crack Propagation and (c) Close-up View of Plastic Strain Contours for Model With Curve 1 Material Properties Using Plastic Strain as Removal Criterion ( $a/W = 0.45$ ) .....	19
Figure 4.6: (a) Plastic Strain Contours, (b) Crack Propagation and (c) Close-up View of Plastic Strain Contours for Model With Curve 1 Material Properties Using Plastic Strain as Removal Criterion ( $a/W = 0.5$ ) .....	20
Figure 4.7: (a) Plastic Strain Contours, (b) Crack Propagation and (c) Close-up View of Plastic Strain Contours for Model With Curve 2 Material Properties Using Plastic Strain as Removal Criterion ( $a/W = 0.4$ ) .....	21
Figure 4.8: (a) Plastic Strain Contours, (b) Crack Propagation and (c) Close-up View of Plastic Strain Contours for Model With Curve 2 Material Properties Using Plastic Strain as Removal Criterion ( $a/W = 0.45$ ) .....	22
Figure 4.9: (a) Plastic Strain Contours, (b) Crack Propagation and (c) Close-up View of Plastic Strain Contours for Model With Curve 2 Material Properties Using Plastic Strain as Removal Criterion ( $a/W = 0.5$ ) .....	23
Figure 4.10: (a) Plastic Strain Contours, (b) Crack Propagation and (c) Close-up View of Plastic Strain Contours for Model With Curve 3 Material Properties Using Plastic Strain as Removal Criterion ( $a/W = 0.4$ ) .....	24
Figure 4.11: (a) Plastic Strain Contours, (b) Crack Propagation and (c) Close-up View of Plastic Strain Contours for Model With Curve 3 Material Properties Using Plastic Strain as Removal Criterion ( $a/W = 0.45$ ) .....	25
Figure 4.12: (a) Plastic Strain Contours, (b) Crack Propagation and (c) Close-up View of Plastic Strain Contours for Model With Curve 3 Material Properties Using Plastic Strain as Removal Criterion ( $a/W = 0.5$ ) .....	26
Figure 4.13: (a) Plastic Strain Contours, (b) Crack Propagation and (c) Close-up View of Plastic Strain Contours for Model With Curve 1 Material Properties Using Strain Energy Density as Removal Criterion ( $a/W = 0.4$ ) .....	27

## List of figures (continued)

---

Figure 4.14: (a) Plastic Strain Contours, (b) Crack Propagation and (c) Close-up View of Plastic Strain Contours for Model With Curve 1 Material Properties Using Strain Energy Density as Removal Criterion ( $a/W = 0.43$ ).....	28
Figure 4.15: (a) Plastic Strain Contours, (b) Crack Propagation and (c) Close-up View of Plastic Strain Contours for Model With Curve 2 Material Properties Using Strain Energy Density as Removal Criterion ( $a/W = 0.4$ ).....	29
Figure 4.16: (a) Plastic Strain Contours, (b) Crack Propagation and (c) Close-up View of Plastic Strain Contours for Model With Curve 2 Material Properties Using Strain Energy Density as Removal Criterion ( $a/W = 0.45$ ).....	30
Figure 4.17: (a) Plastic Strain Contours, (b) Crack Propagation and (c) Close-up View of Plastic Strain Contours for Model With Curve 2 Material Properties Using Strain Energy Density as Removal Criterion ( $a/W = 0.5$ ).....	31

## List of tables

---

Table 2.1: Standard DT Specimen Configuration Dimensions.....	4
Table 2.2: Material Test Data to be Used in Analyses.....	4
Table 4.1: Summary of FE Results - Shear-Lip Sizes for 25 mm Thick Specimen.....	16

## **Acknowledgements**

---

The authors would like to acknowledge the contributions of Dr. E.C. Oguejiofor of St. Francis Xavier University, Antigonish, NS.



## **1. INTRODUCTION**

### **1.1 Background**

A major component of the DRDC Atlantic Dockyard Laboratory (DRDC/Atlantic DL) fracture control program is linking large specimen size dynamic tear (DT) transition curves to structural transition curves and quantitative fracture parameters. To do this it is necessary to determine relationships between stretch zone and plastic zone size before crack advance and plastic zone size at and just after crack advance and the size of the developing shear-lip. The former relationship, that between stretch zone and plastic zone, has been investigated in previous studies resulting in a relationship of plastic zone to stretch zone of 80 to 100. In several papers going back to 1991, DRDC Atlantic DL has estimated that the shear-lip (actual shear-lip width plus specimen contraction) that develops is approximately equal to the mid specimen plastic zone at crack advance.

### **1.2 Objectives and Scope**

The objective of this study is to demonstrate the feasibility of a numerical simulation of shear-lips for a base metal quasi-static loading rate dynamic tear (DT) specimen three-point bend test. Three real stress-real strain curves acquired for gauge lengths of 1.25 mm (0.050 inches) supplied by DRDC/DL will be used for the model. Crack advance and element or node release will be based on two possible criteria. The two criteria are (a) when the average strain in the crack tip elements that occupy a physical surface of 1.25 mm (0.050 inches) exceeds the strain at fracture on the supplied data; and (b) when the strain energy density in elements occupying a volume defined by 1.25 mm (0.050 inches) of free surface at the crack tip and 1.25 mm (0.050 inches) of material depth exceeds the strain energy density calculated from the supplied real stress real strain curves.

## **2. PROBLEM DESCRIPTION**

### **2.1 Specimen Configurations**

A schematic representation of the test specimen is presented in Figure 2.1. The specimen dimensions are presented in Table 2.1. The specimen is made of 350WT steel material.

### **2.2 Description of Shear-Lip and Plastic Zone in DT Specimens**

Figure 2.3 shows schematically the plastic zone associated with the DT specimen. In this figure  $S_{zw}$  is the stretch zone width and  $r_y$  is the plastic radius. Figure 2.4 is a schematic of the crack front of a standard DT specimen showing the shape of the shear-lip,  $S$ . The shear index can be calculated using Equation 2.1, where  $SI$  is the shear index,  $S$  is the shear-lip and  $B$  is the specimen width (25mm for this study). [4]

$$SI = \frac{2S}{B} \quad \text{Equation 2.1}$$

### **2.3 Requirements**

It is required to model the shear-lip formation and plastic zone development by finite element technology for 25 mm standard DT specimens with cracks extended to 14 mm by fatigue as the starting point. Three different 1.25mm gage length real stress real strain curves will be used to model the material behaviour and define element or node release. Formation of the crack and subsequent shear-lips at  $a/W$  of 0.4, 0.5, and 0.6, will be compared to the plastic zone at crack initiation and at .050 inch crack extension. The specific goals of the study include:

1. Analysis of the three real stress-real strain curves for the data supplied to determine the strain energy density for each.
2. Review of three available approaches for modeling the crack advance - element removal, remeshing and node release, to determine which one is most appropriate to use in conjunction with the FE program chosen.
3. Development of FE models for the 25 mm DT specimen configuration, model element release based on strain to fracture and strain energy density and determine the shear-lip formation for each data set and each failure criteria. These results will be used to demonstrate the sensitivity of the simulated shear-lip size to the modeling parameters and

failure criteria.

4. Provide results in tabular and/or graphical form to display the essential relationship of plastic zone at initiation of crack advance and plastic zone at 1.25mm crack advance and the developing shear-lip at  $a/W$  of 0.4 0.5 and 0.6.
5. Provide motion clips for viewing dynamically these results.
6. Documentation of results in a contractor report.

The material test data to be used (1.25mm gage length real stress-real strain data) is presented in Table 2.2 and Figure 2.2. Curve 1 represents the complete real stress-real strain behaviour, with the failure strain at 206% and yield stress at 394MPa. Curve 2 is similar to Curve 1 except that the failure strain is 103%, which is half of the Curve 1 value. Similarly, Curve 3 is the case with the failure strain the same as Curve 1 but with the yield stress equal to 197MPa, which is half of the Curve 1 value. As stated before, these will be used to study the sensitivity of the shear-lip size to the modelling parameters and failure criteria.

Table 2.1: Standard DT Specimen Configuration Dimensions

Dimensions	Specimen (DT-350WT-25)
Beam Length, L (mm)	181
Beam Span, S (mm)	164
Crack Length, a (mm)	14*
Beam Width, W (mm)	41
Beam Thickness, B (mm)	25

\*a = 12 mm plus 0.254 mm pressing followed by fatigue extension to 14 mm

Table 2.2: Material Test Data to be Used in Analyses

Strain (mm/mm)	Stress (MPa)		
	Curve 1	Curve 2	Curve 3
0	395	395	197
0.0133	509	509	255
0.3330	650	650	325
1.0000	820	820	410
1.0300	820	374	410
1.0310	820	2.4	410
1.6600	949		475
2.0000	949		475
2.0600	374		187
2.0610	2.4		1.2

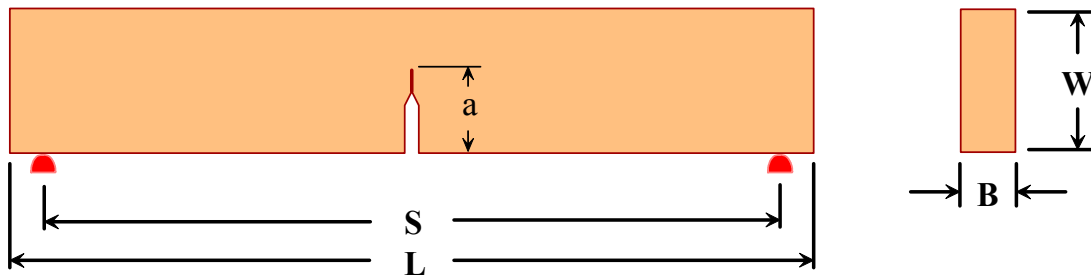


Figure 2.1: Configuration of DT Specimen

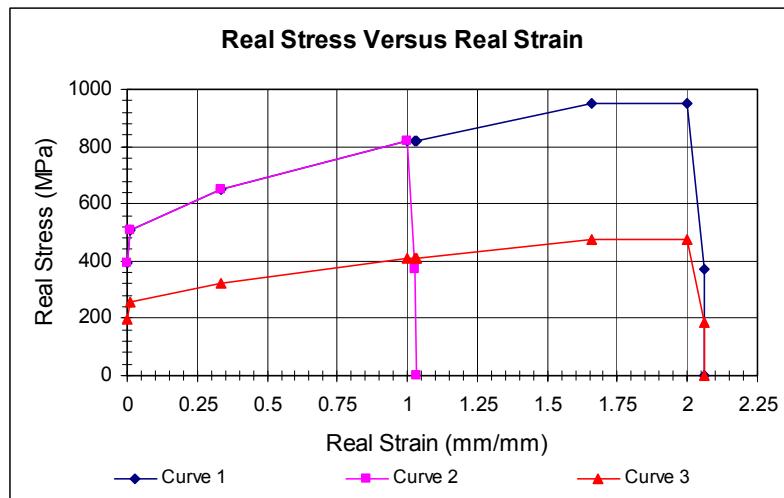


Figure 2.2: Graphical Representation of Material Test Data to be Used in Analyses

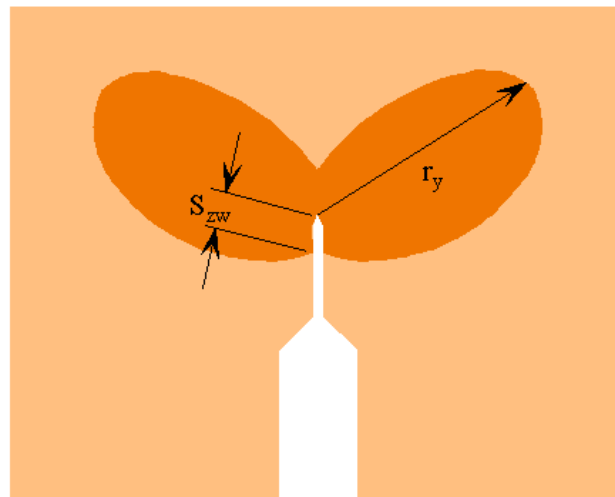


Figure 2.3: Schematic of DT Specimen Showing Plastic Zone

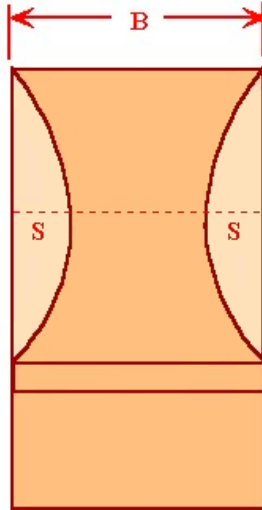


Figure 2.4: Schematic of Cross-Section of DT Specimens Showing Shear-Lip Formation

### **3. FINITE ELEMENT MODEL**

#### **3.1 Finite Element Approach**

Several different methods of simulating crack advance in a finite element model have been investigated, including remeshing, node release and element removal [5]. Consideration was given to both ABAQUS [6] and ANSYS [7] and finite element packages to perform the analysis needed for this study. Due to the complexity and the computation effort required, it was concluded that the method of remeshing would not be considered in this study. Initially, both element removal and node release were considered in the ANSYS environment. Focus was placed on the method of node release. This process required a fairly high degree of computational effort due to the requirement of fairly small mesh sizes. If the mesh were too coarse, the solution would begin to diverge.

Due to difficulties experienced using ANSYS, focus was shifted to the ABAQUS. The method of element removal using the MODEL CHANGE option in ABAQUS was considered. The software also has a wide range of non-linear materials models and can account for large strains and displacements. Initial testing of this software for this procedure was very promising, therefore, the ABAQUS finite element software was used to model the elastic-plastic behaviour of the Standard DT specimen. However, for convenience, the HyperMesh [4] general-purpose pre- and post-processing program was used for model generation and results processing.

##### **3.1.1 Element Removal Process in ABAQUS**

Figure 3.1 shows a flow chart outlining the procedure adopted to perform the crack propagation analyses. An external program, written in the Fortran language, is used to automate iterative removal process. This program starts the ABAQUS runs and then reads the ABAQUS ASCII result files once an analysis step is complete and determines if any nodes or elements on the crack front have exceeded the specified criteria for crack growth (plastic strain or strain energy density). If any nodes have failed the criteria, the program generates and runs a removal step containing any elements in the crack front connected to those nodes. The ASCII results file is read after this removal step to determine if any nodes or elements still exceeded the crack growth criteria. If there are additional elements to be removed another removal step is performed. Otherwise the load is incremented and the removal process is repeated. This process is continued

until all of the elements in the crack front have been removed, until a specified maximum load has been attained or a specified maximum number of steps has been performed.

### **3.2 Finite Element Meshes**

The HyperMesh software was used to generate the finite element models of the DT standard specimens, which were then translated to ABAQUS input files. Several finite element models were generated to determine a mesh refinement, which minimized computational effort but did not diminish quality of the results. The model selected is shown in Figure 3.2(a) and (b). This is a doubly symmetric model (about longitudinal and transverse axis) and contains 4450 8-node brick elements and 5446 nodes. The elements to be removed in the crack front are  $0.683 \times 0.625 \times 0.25 \text{ mm}$ , which will allow the crack to propagate  $0.683 \text{ mm}$  ( $0.027 \text{ in}$ ) at a time.

It should be noted that the problem being solved is a highly non-linear one that required enormous computational time and data storage requirements. For these reasons, the mesh size and configuration had to be limited to the one shown in Figure 3.2. With this model, a typical run requires 2-3 days and 1.0-2.0 GB of data storage. To further reduce the storage requirements, only stress/strain results on only the elements in the crack face.

### **3.3 Material Models**

An incremental rate independent plasticity theory available in the ABAQUS finite element program [3] was used for the material constitutive model. This standard model for plasticity is summarized in the Phase I report [1]. As previously mentioned, three different representations of stress-strain behaviour of 350 WT steel material are considered. These curves were presented in Table 2.2 and Figure 2.2.

### 3.4 Boundary Conditions and Loading

The following boundary conditions were applied:

At the support:  $y = 0$

Along the longitudinal centre line:  $z = 0$

Along the transverse centre line:  $x = 0$ ;

where,  $x, y$  and  $z$  are the displacements components in the longitudinal, transverse and out of plane directions, respectively. The boundary conditions are displayed in Figure 3.3.

The load is applied as a pressure load distributed across a 8mm section at the top of the coupon (darkest elements in Figure 3.2) as shown in Figure 3.3.

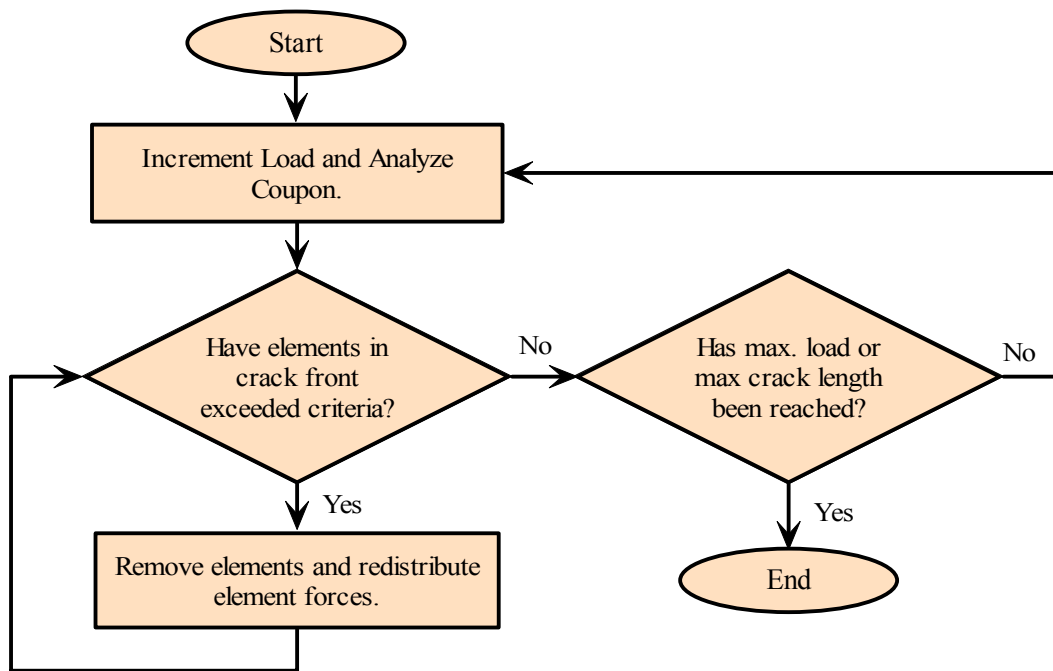


Figure 3.1: Flow Chart Showing the Procedure Used for Element Removal in ABAQUS Environment

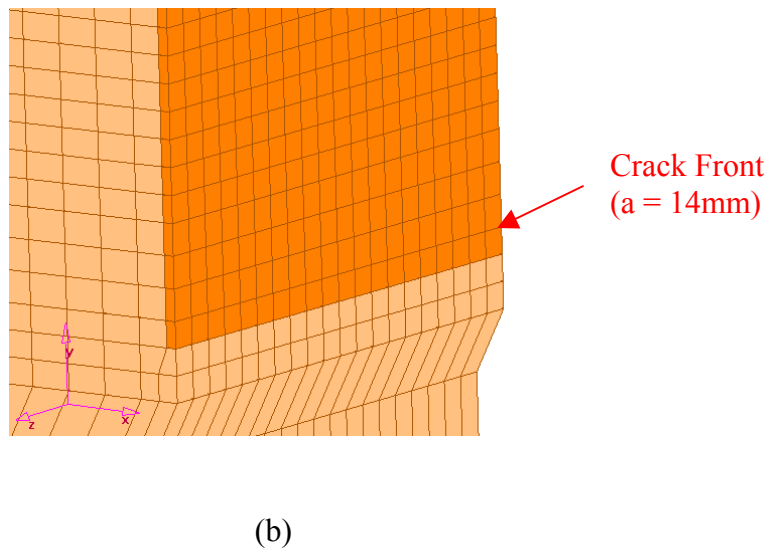
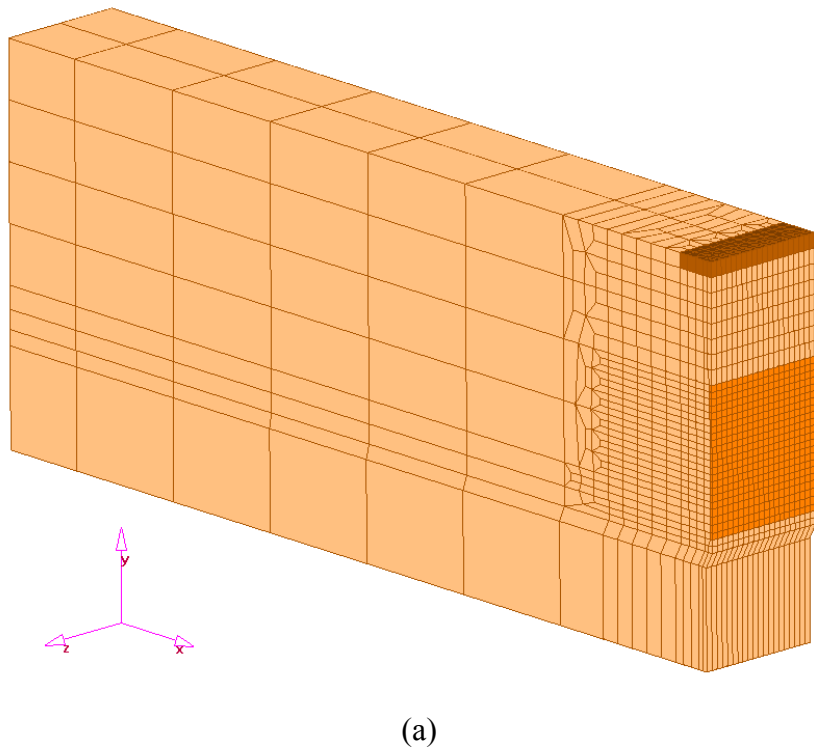


Figure 3.2: Finite Element Mesh of Standard DT Specimen

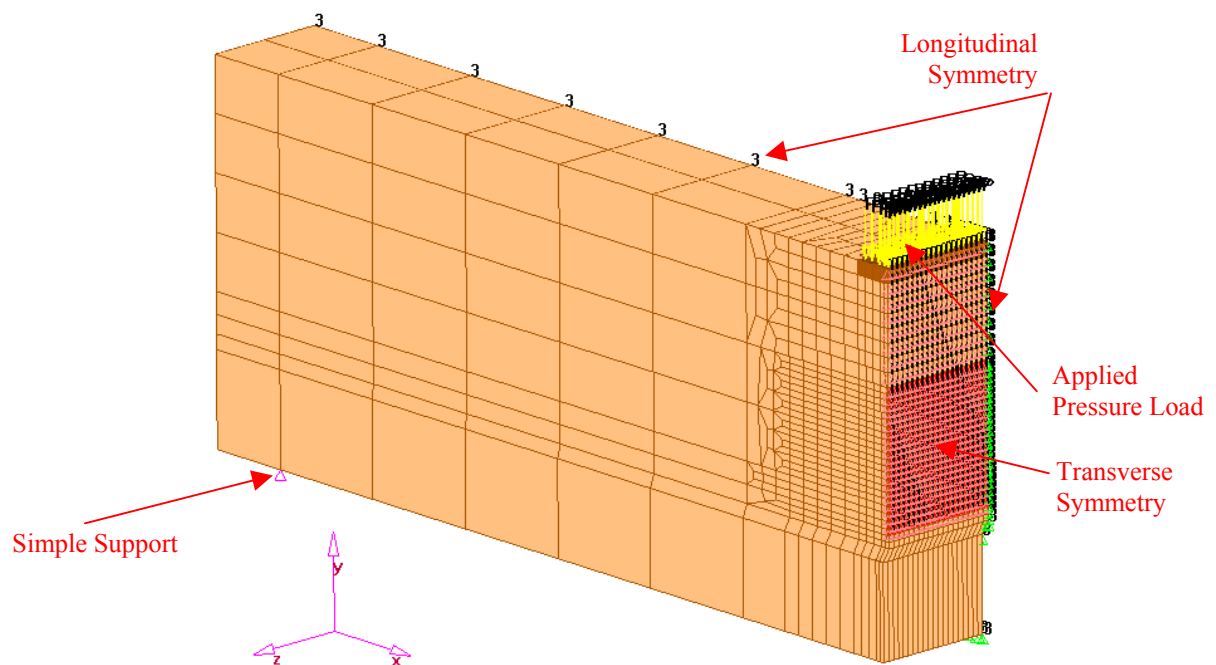


Figure 3.3: Finite Element Model of Standard DT Specimen Showing Applied Loading and Boundary Conditions

## **4. RESULTS AND DISCUSSIONS**

### **4.1 Strain Energy Densities for the Three Curves**

The three real stress real strain curves provided were analysed and the corresponding strain energy densities were determined as follows (by calculating the area under the stress vs strain curves):

Curve 1 – 1625 N mm/mm<sup>3</sup>

Curve 2 - 700 N mm/mm<sup>3</sup>

Curve 3 - 813 N mm/mm<sup>3</sup>

These results are used as the criteria value for element removal using strain energy density.

### **4.2 Shear-Lip and Plastic Zone Development with Maximum Strain Criteria**

During the analysis process a computer disk space problem was encountered. When storing results for all of the elements in the model for each analysis step, the result file sizes were quickly exceeding 1.0GB. It was determined that there was no significant advantage to retaining results for any elements outside of those in the plane of the crack front. Figure 4.1 shows the plastic strain contours at a displacement level of  $D_L = 6.29\text{mm}$ . As can be seen in this figure, the plastic zone resulting from the crack front can no longer be distinguished. This plastic zone merges with the yielded region from the load after a displacement of approximately 1mm. For this reason, results are only printed for elements in the plane of the crack front (darker elements in Figure 4.2).

Figure 4.3 shows the process used to determine the shear-lip size,  $S$  from the finite element analysis. As illustrated in the figure, the shear-lip occurs as a result of the so-called tunnelling effect where the crack grows faster in the centre of the specimen as a result of higher stress triaxiality in the centre than at the edges. Thus the material tends to break at the centre while the edges try to hold on. The shear-lip size,  $S$  is given by the largest distance from the edge of the specimen to the edge of the fractured surface (“tunnel”) in the centre of the specimen. To obtain the shear-lip size from the finite element analysis, plastic strain contours of the crack face are plotted for each case. The fractured surface corresponds to the region with very high plastic strains shown as the red contours in the figures that follow. The shear-lip is measured from the specimen edge to the point where the high strain contours plateau out near the specimen centre, as

shown. This process was shown to provide the most consistent and reasonable set of results. However, in some cases, it was difficult to measure this distance due to big jumps in contours obtained, and judgement had to be employed in determining the shear-lip size. These cases are highlighted in the discussions below.

Figure 4.4 shows the plastic strain contours and the corresponding location of the crack front (degree of element removal) for the case using Curve 1 material definition and a plastic strain of 200% as the removal criterion. Figure 4.4(a) shows the plastic strain contours on the crack face and Figure 4.4(b) shows the elements removed when the crack front has reached an  $a/W$  value of 0.4. Figure 4.4(c) shows a close-up view of the plastic strain contours that are used to estimate the shear-lip size. Figures 4.5 and 4.6 show the corresponding plots for the cases when the crack front level reached  $a/W$  values of 0.45 and 0.5, respectively. Unfortunately, due to convergence problems, the analysis could not be continued to  $a/W = 0.6$ .

Figure 4.7 to 4.9 show the results for the case using Curve 2 material definition and a plastic strain of 100% as the removal criterion. Figure 4.10 to 4.12 show the results for the case using Curve 3 material definition and a plastic strain of 200% as the removal criterion.

The shear-lip size(s) obtained for the three material curves are summarized in Table 4.1. The corresponding shear indices ( $SI = 2S/B$ ) are also presented in the table, where  $B$  is the specimen thickness. At any given crack size ( $a/W$  level), the shear-lip size is smallest for Curve 2 material and largest for Curve 3. This trend seems reasonable as the Curve 2 material is the most brittle (100% strain to failure as opposed to 200% strain for Curves 1 and 3); and the Curve 3 material is the most plastic (has lower yield stress of 197MPa compared to 395MPa for Curves 1 and 2, and high failure strain of 200%). For a given material (Curve 1 for example), the shear-lip size tends to reduce with increasing crack size. For instance, for the Curve 1 material, the shear-lip sizes for  $a/W = 0.4$ , 0.45 and 0.5 are 10.95mm, 10.30mm and 9.70mm, respectively. This observation is consistent with earlier DRDC – Atlantic studies [4] in which it was shown that the shear-lip size and hence shear index ( $SI$ ) was related to the fracture energy. The specimens with larger size cracks required smaller fracture energy and hence smaller shear-lip sizes. A similar trend is generally observed for the Curves 2 and 3 materials, although some discrepancies occurred at  $a/W = 0.4$  for Curve 2 and at  $a/W = 0.45$  for Curve 3. These are some of the cases for which it was difficult to measure the shear-lip sizes precisely, as discussed above.

### 4.3 Shear-Lip Development with Strain Energy Density Criteria

The use of the strain energy density criterion presented some difficulties with regards to convergence of the solution. This was probably because of the fact that the fracture criterion was based on the uniaxial, rather than the triaxial strain energy density; and also due to the rather large element sizes (about 0.683x0.625x0.25mm) in the fracture face. Fracture usually occurred at higher strain levels than the fracture strains, hence the stress-strain curve had to be extended somewhat beyond the fracture strain, to achieve convergence. Due to these difficulties as well as time and budget constraints it was not possible to complete all of the cases planned. Only analysis for Curves 1 and 2 were performed.

Figures 4.13 to 4.14 show the plastic strain contours, the corresponding location of the crack front and close-up views of the strain contours for the case using Curve 1 material definition, using a strain energy density of 1625 N mm/mm<sup>3</sup> as the removal criterion, when the crack front has reached  $a/W$  of 0.4 and 0.45, respectively. Figures 4.15 to 4.17 show the corresponding cases for the Curve 2 material, using a strain energy density of 700 N mm/mm<sup>3</sup> as the removal criterion, when the crack front has reached  $a/W$  of 0.4, 0.45 and 0.5, respectively.

The shear-lip sizes obtained for these cases are also summarized in Table 4.1, where the corresponding shear indices are also presented. Again, the shear-lip sizes are smaller for the more brittle material (Curve 2) than the more plastic material (Curve 1). For instance, at  $a/W = 0.4$ , the shear-lip sizes for the Curve 2 and Curve 1 materials are 11.90mm and 8.10mm, respectively. Furthermore, for a given material the shear-lip size decreases with increase in crack size. Consider, for instance, the case of the Curve 1 material. The shear-lip size varied from 11.90mm at  $a/W = 0.4$  to 11.20mm at  $a/W = 0.45$ . However, this trend is not very precise with the Curve 2 material.

From Table 4.1, it is seen that for any given material and crack size, the shear-lip size predicted based on the strain energy density criterion is greater than the predicted based on the plastic strain criterion. As discussed above, this is probably due to the strain-energy density being obtained from uniaxial testing rather than a triaxial test, such that fracture occurred at higher strain levels than the fracture strain. A more refined approach will be to use strain energy density obtained from material tested in a triaxial state of stress that is closer to the state of stress in the DT specimen.

Table 4.1: Summary of FE Results - Shear-Lip Sizes for 25 mm Thick Specimen

a/w	Property	Curve 1		Curve 2		Curve 3	
		Strain Criterion	Strain Energy Criterion	Strain Criterion	Strain Energy Criterion	Strain Criterion	Strain Energy Criterion
0.40	s (mm)	10.95	11.90	7.50	8.10	11.55	-
	SI	0.876	0.952	0.600	0.648	0.924	-
0.45	s (mm)	10.30	11.20	8.70	8.60	10.00	-
	SI	0.824	0.896	0.696	0.688	0.800	-
0.50	s (mm)	9.70	-	6.85	8.60	10.9	-
	SI	0.776	-	0.548	0.688	0.872	-

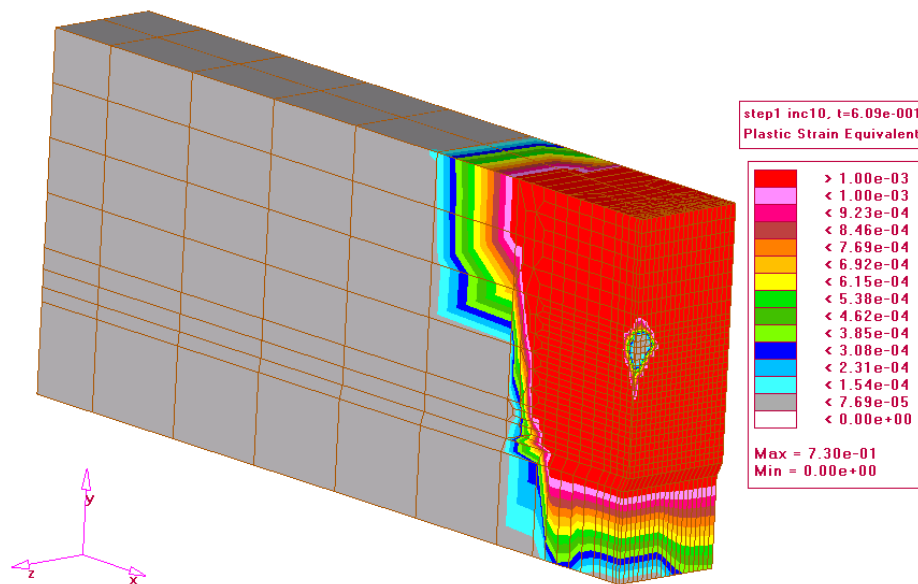


Figure 4.1: Plastic Strain Contours at  $D_L = 6.29\text{mm}$

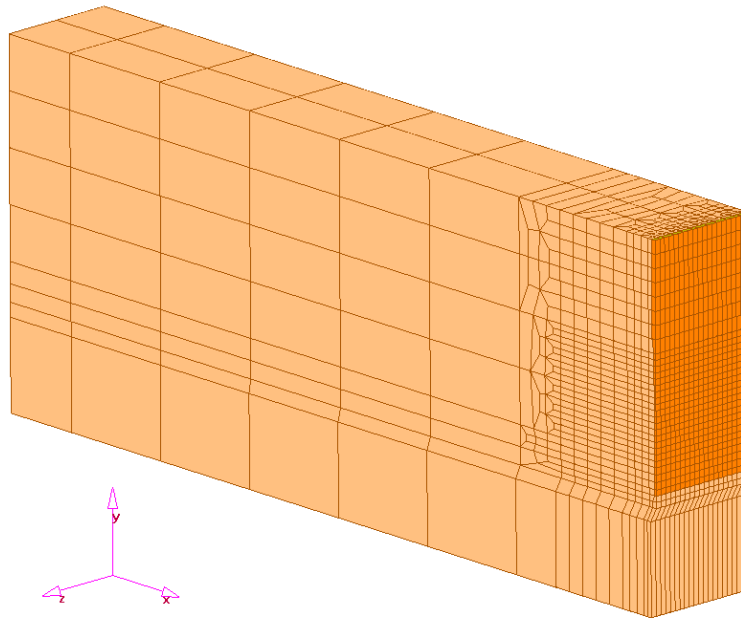


Figure 4.2: Finite Element Mesh Showing Elements For Which Results are Stored

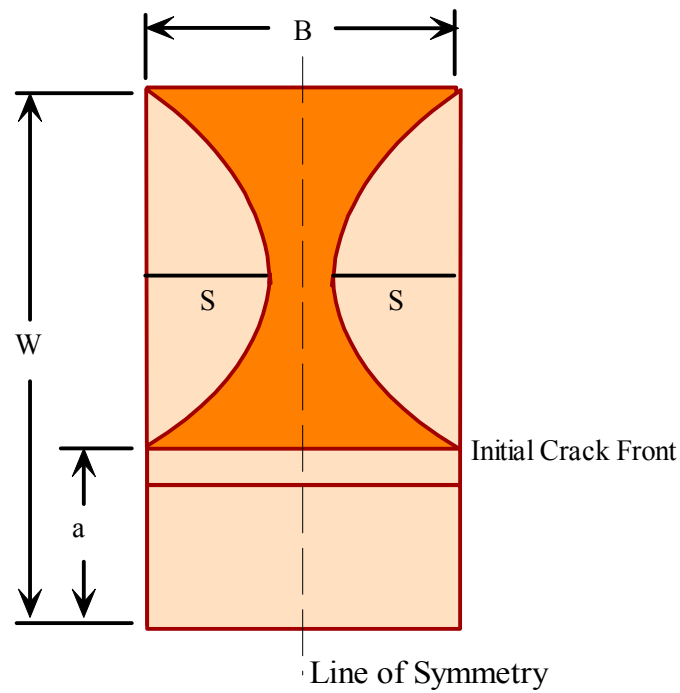


Figure 4.3: Schematic of Crack Face Showing Method of Determining Shear-Lip Size

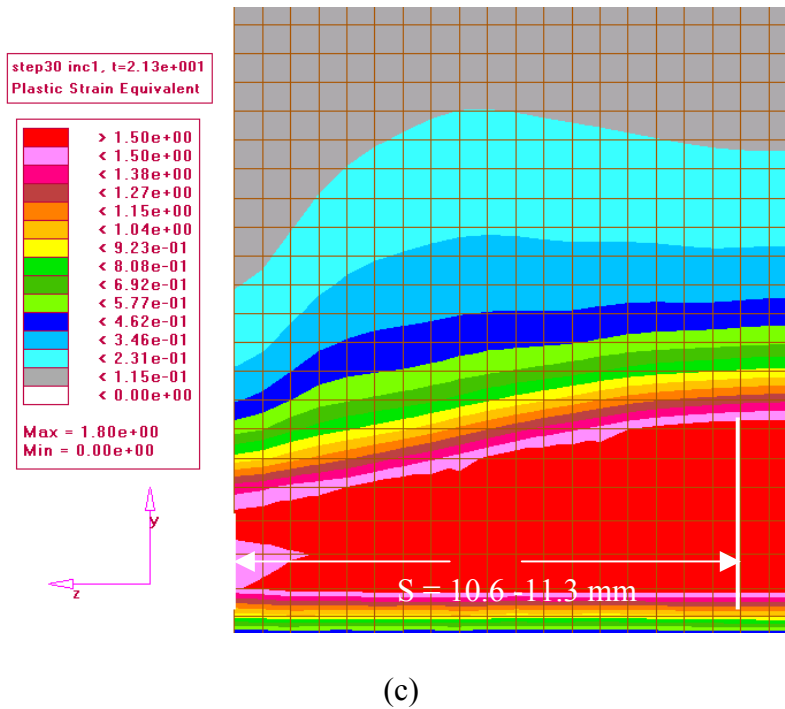
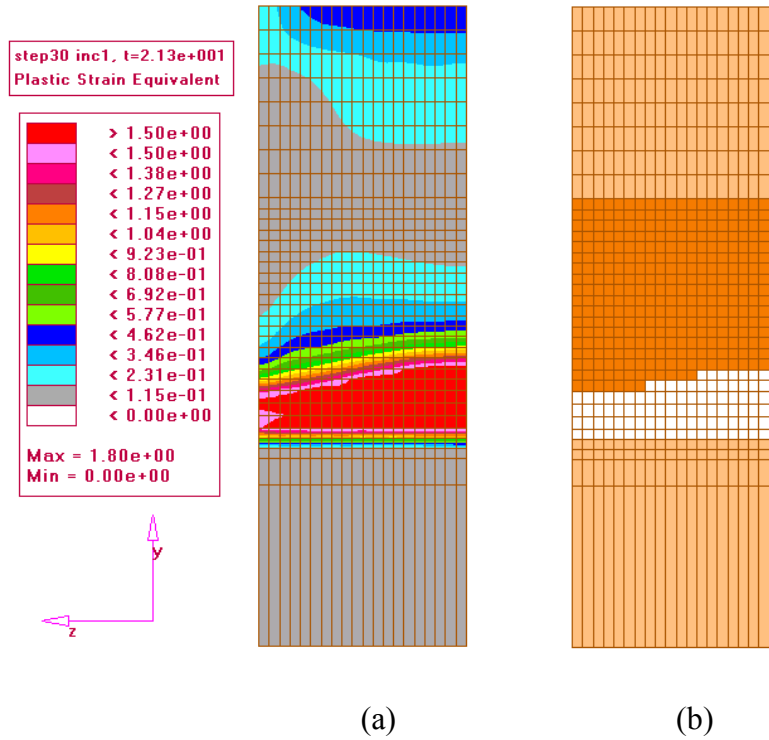


Figure 4.4: (a) Plastic Strain Contours, (b) Crack Propagation and (c) Close-up View of Plastic Strain Contours for Model With Curve 1 Material Properties Using Plastic Strain as Removal Criterion ( $a/W = 0.4$ )

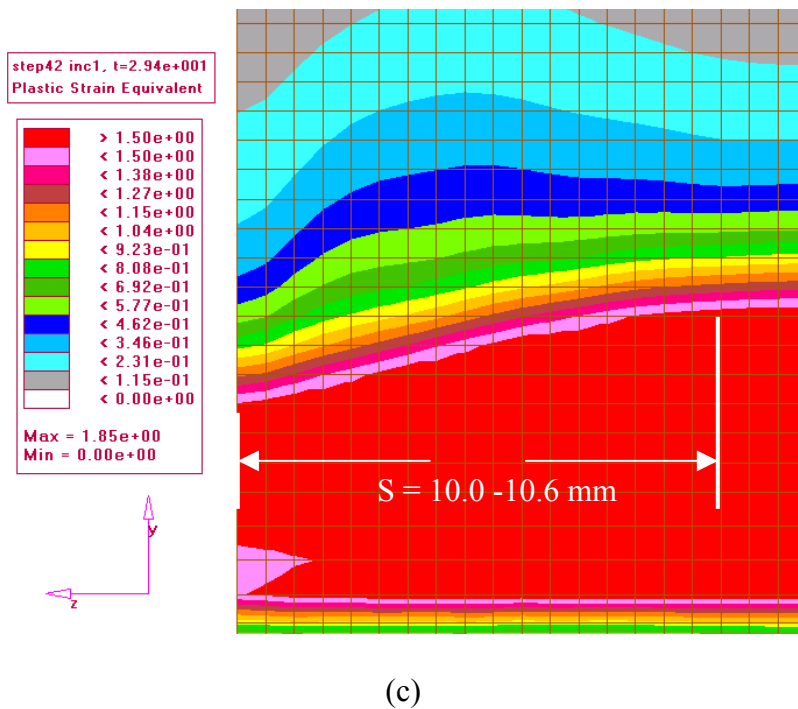
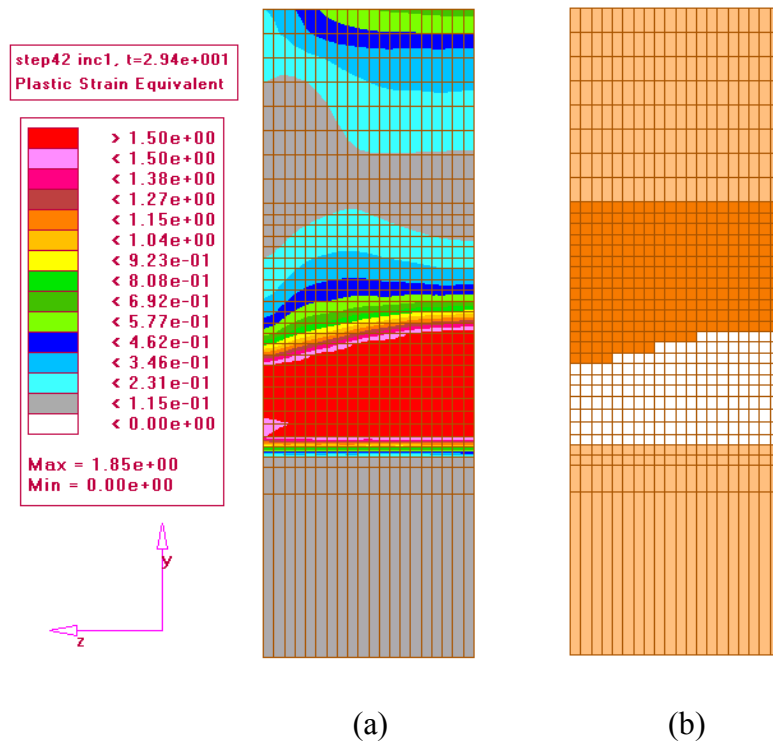


Figure 4.5: (a) Plastic Strain Contours, (b) Crack Propagation and (c) Close-up View of Plastic Strain Contours for Model With Curve 1 Material Properties Using Plastic Strain as Removal Criterion ( $a/W = 0.45$ )

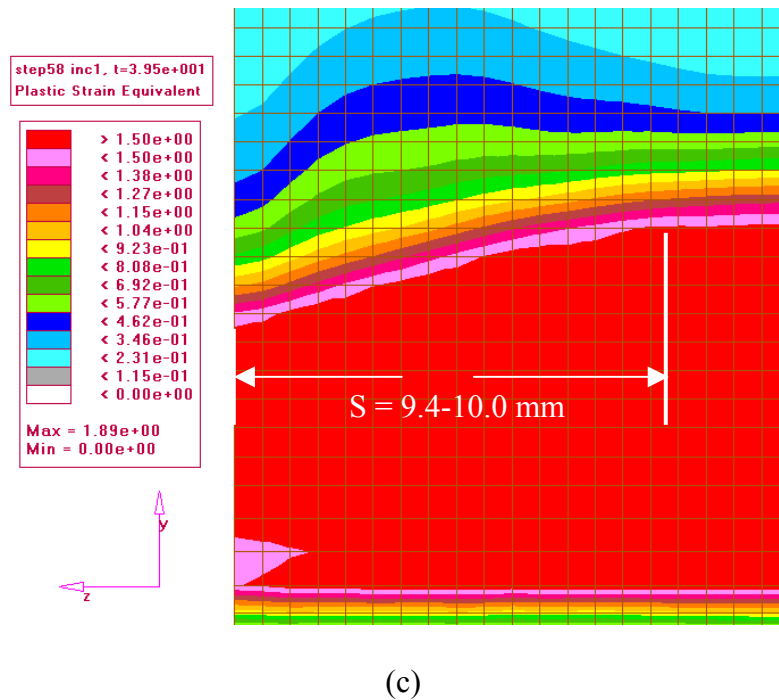
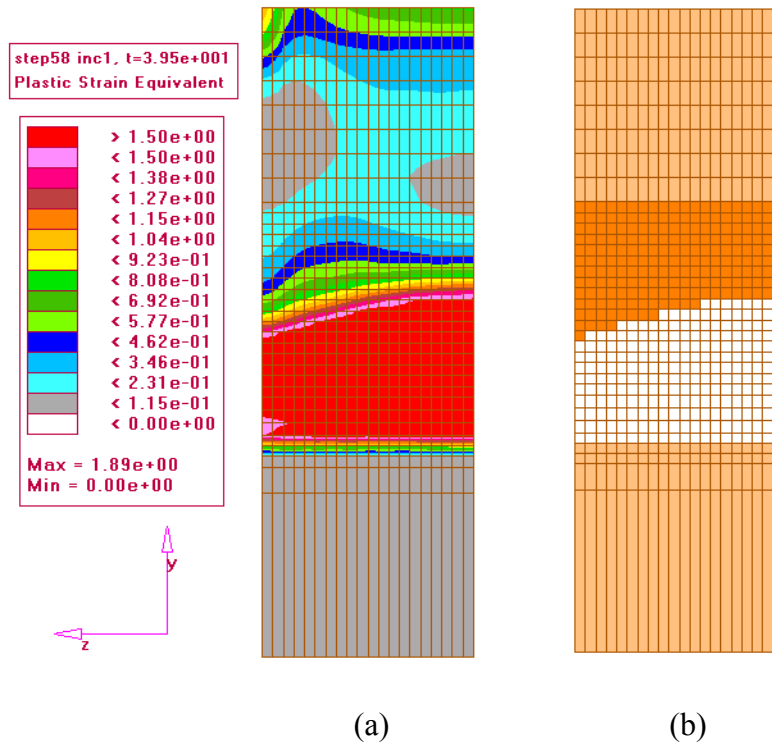


Figure 4.6: (a) Plastic Strain Contours, (b) Crack Propagation and (c) Close-up View of Plastic Strain Contours for Model With Curve 1 Material Properties Using Plastic Strain as Removal Criterion ( $a/W = 0.5$ )

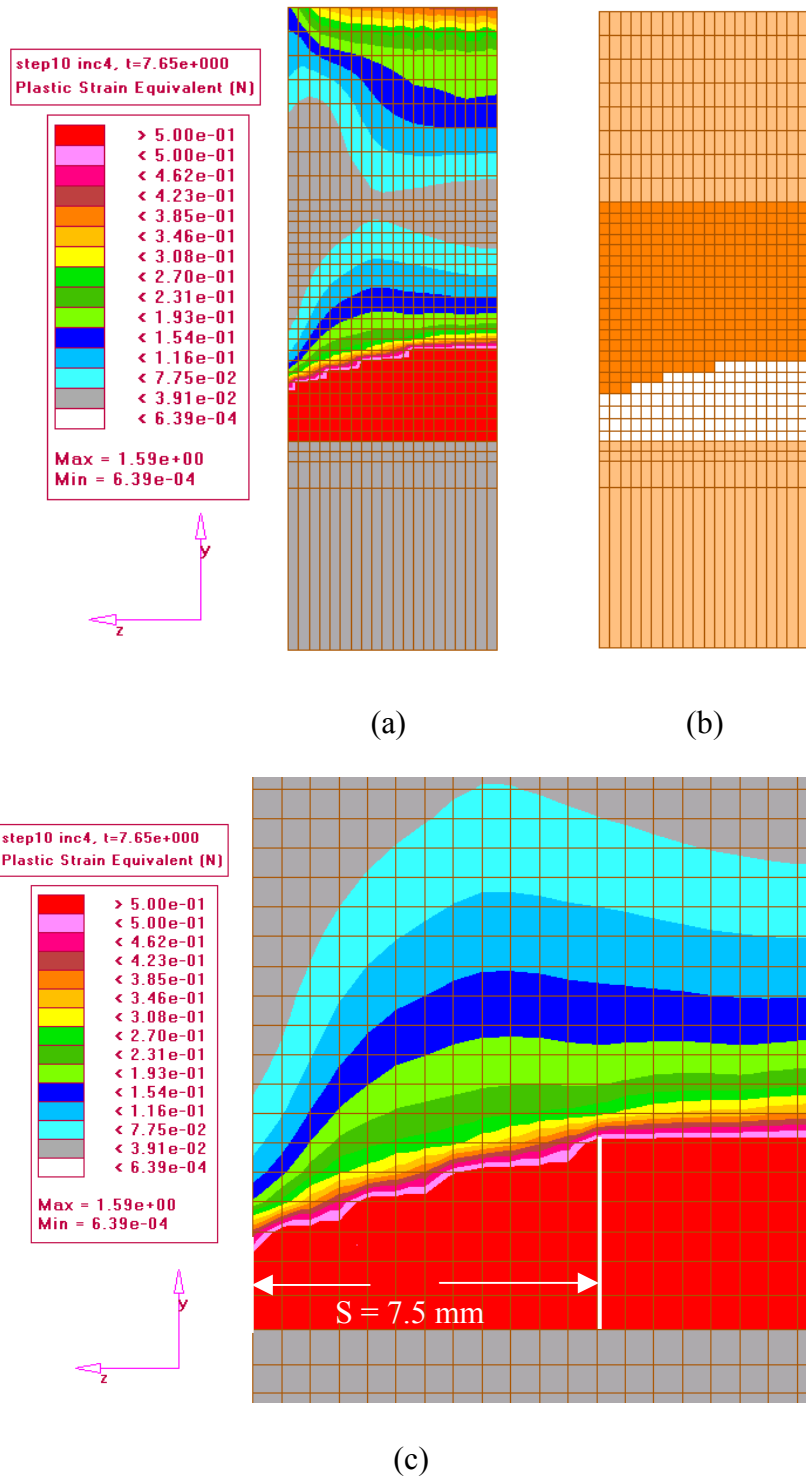


Figure 4.7: (a) Plastic Strain Contours, (b) Crack Propagation and (c) Close-up View of Plastic Strain Contours for Model With Curve 2 Material Properties Using Plastic Strain as Removal Criterion ( $a/W = 0.4$ )

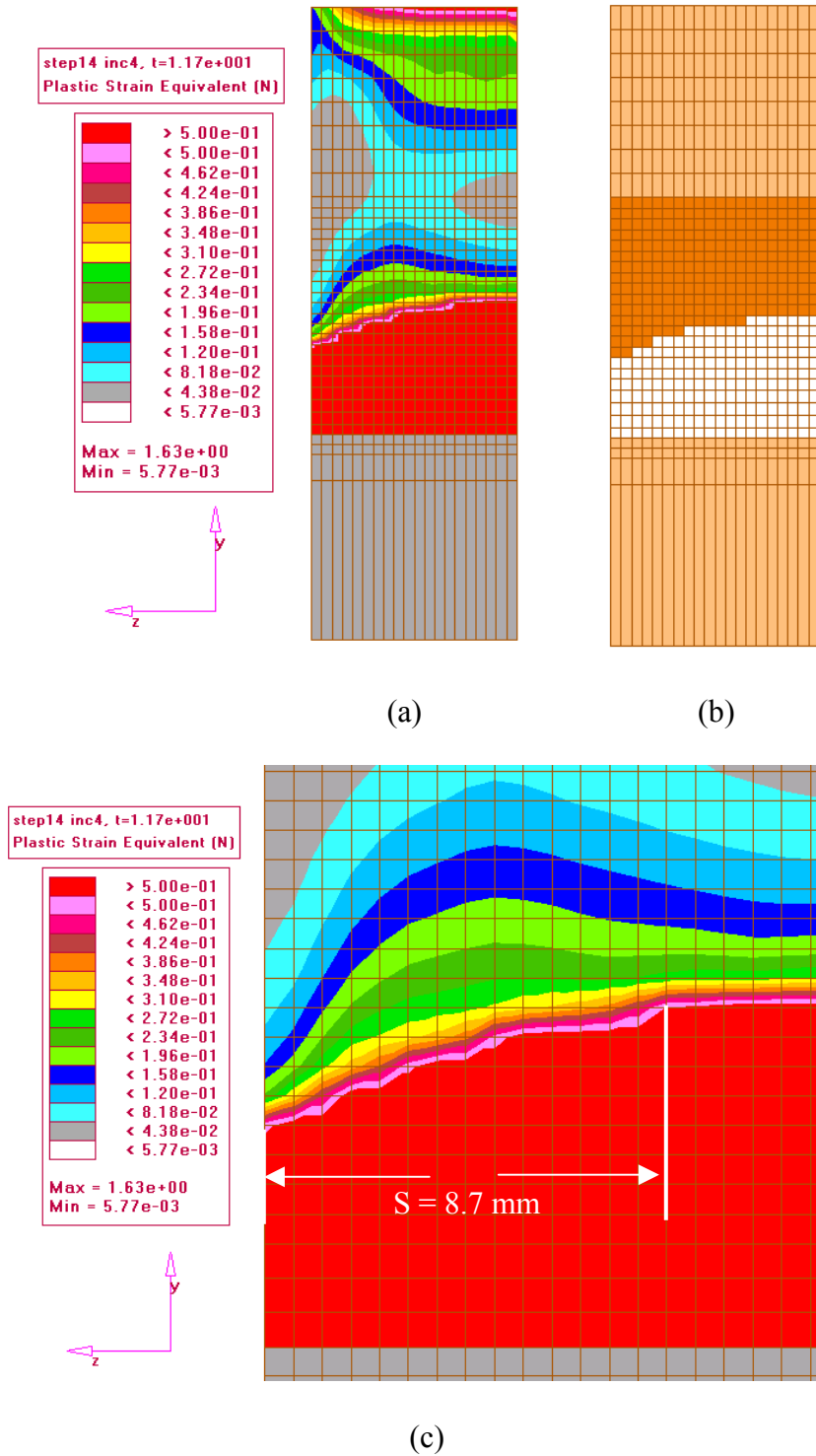


Figure 4.8: (a) Plastic Strain Contours, (b) Crack Propagation and (c) Close-up View of Plastic Strain Contours for Model With Curve 2 Material Properties Using Plastic Strain as Removal Criterion ( $a/W = 0.45$ )

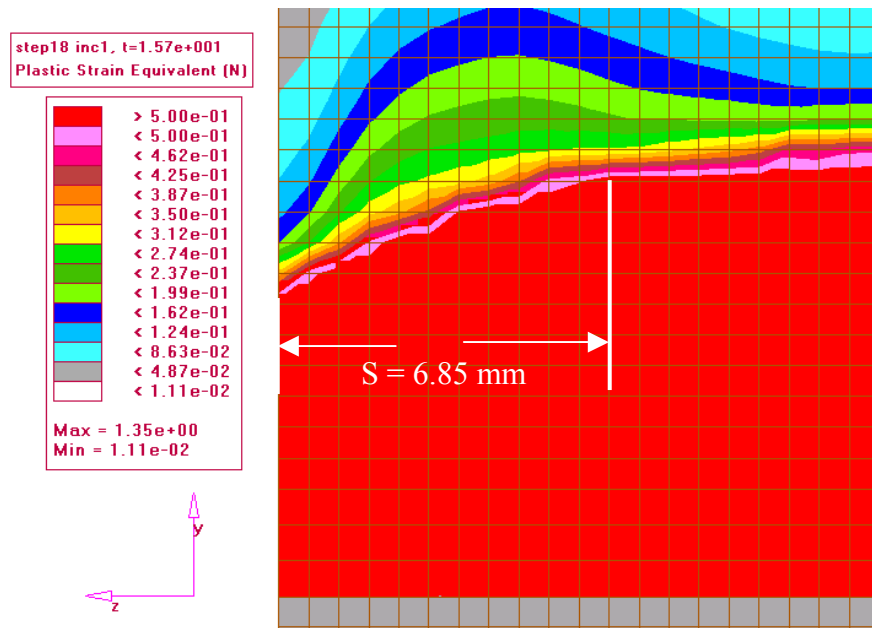
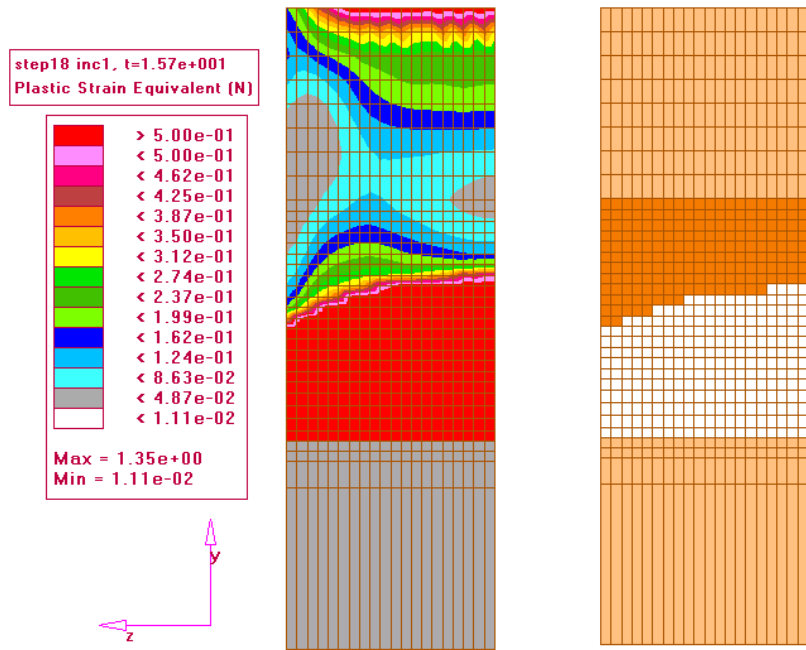


Figure 4.9: (a) Plastic Strain Contours, (b) Crack Propagation and (c) Close-up View of Plastic Strain Contours for Model With Curve 2 Material Properties Using Plastic Strain as Removal Criterion ( $a/W = 0.5$ )

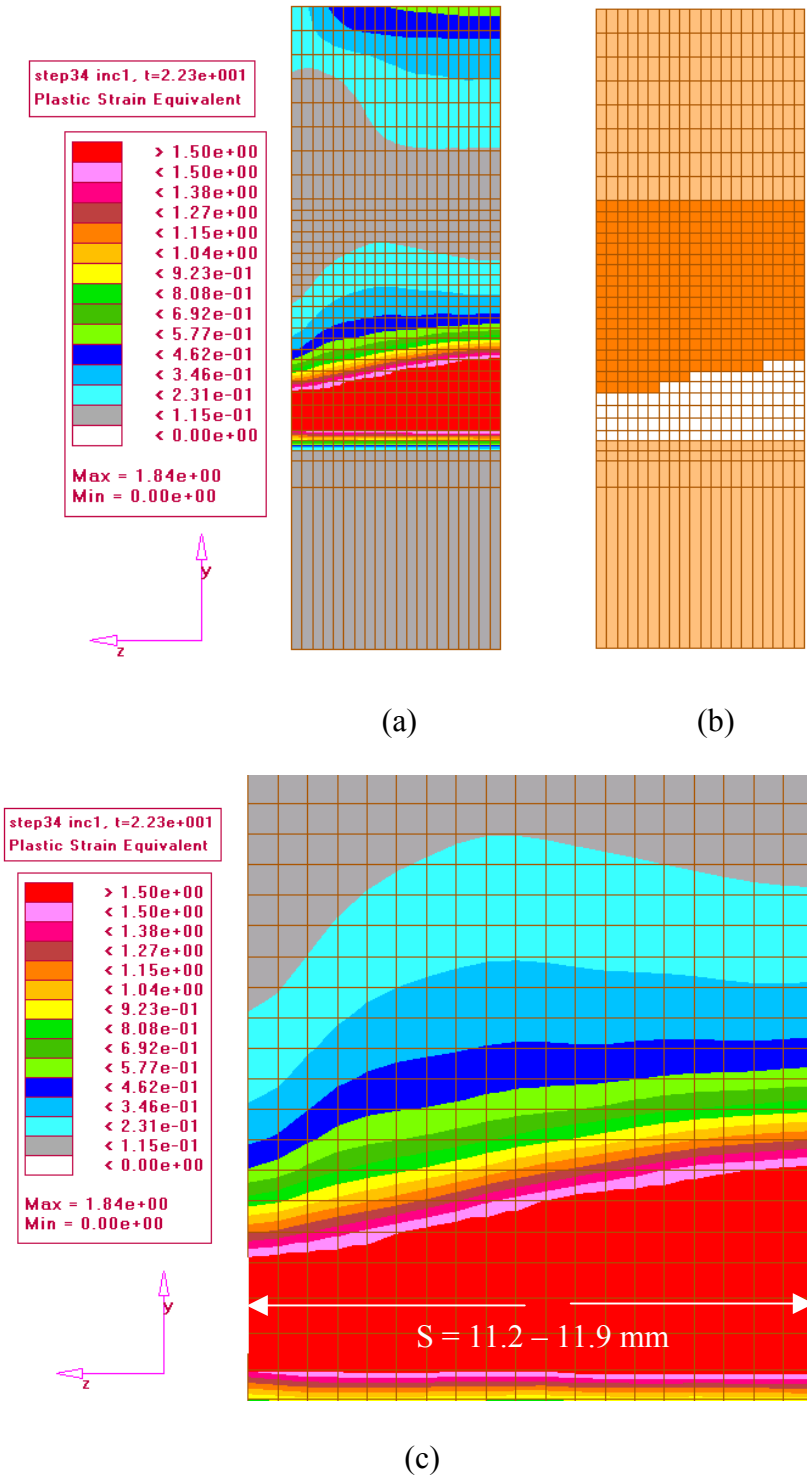


Figure 4.10: (a) Plastic Strain Contours, (b) Crack Propagation and (c) Close-up View of Plastic Strain Contours for Model With Curve 3 Material Properties Using Plastic Strain as Removal Criterion ( $a/W = 0.4$ )

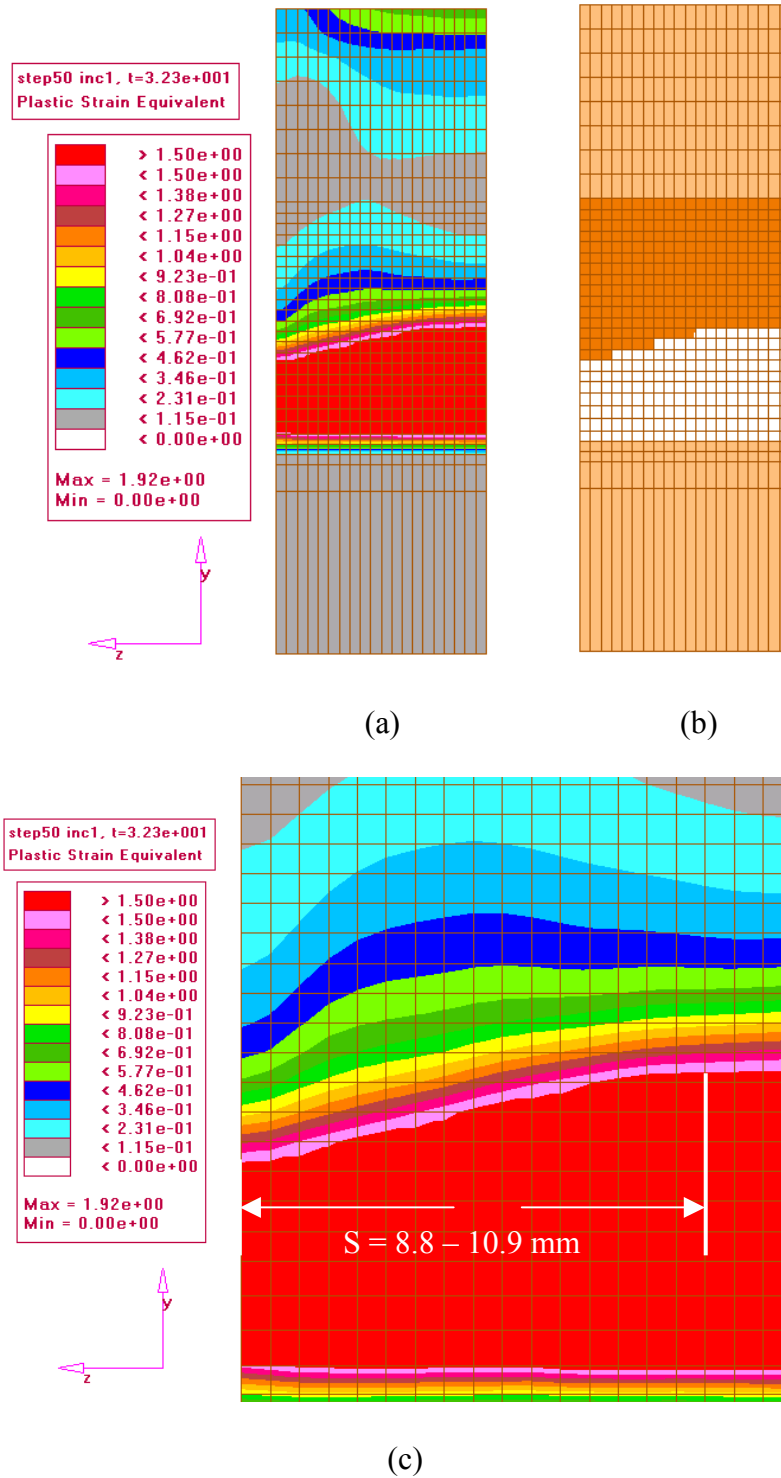


Figure 4.11: (a) Plastic Strain Contours, (b) Crack Propagation and (c) Close-up View of Plastic Strain Contours for Model With Curve 3 Material Properties Using Plastic Strain as Removal Criterion ( $a/W = 0.45$ )

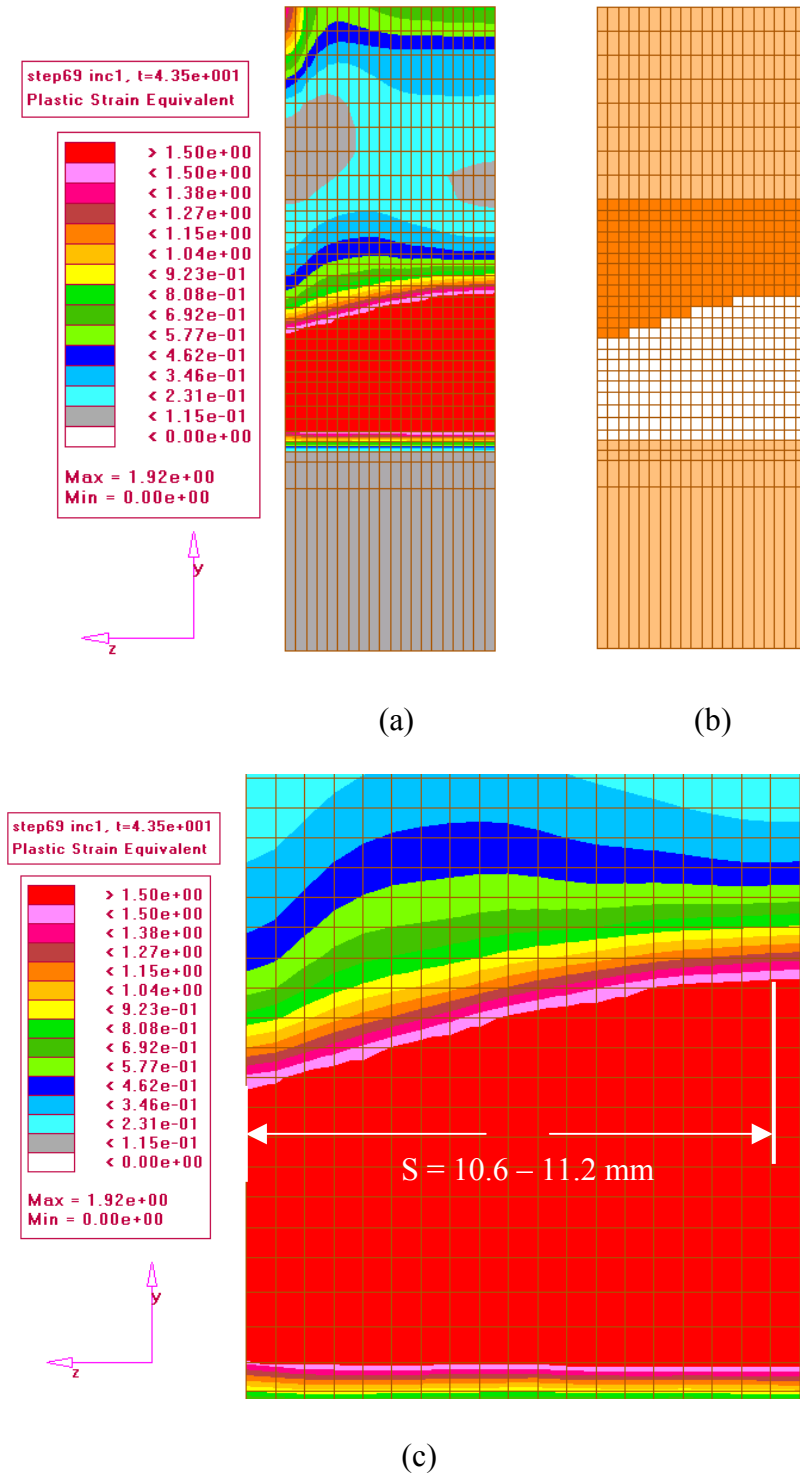


Figure 4.12: (a) Plastic Strain Contours, (b) Crack Propagation and (c) Close-up View of Plastic Strain Contours for Model With Curve 3 Material Properties Using Plastic Strain as Removal Criterion ( $a/W = 0.5$ )

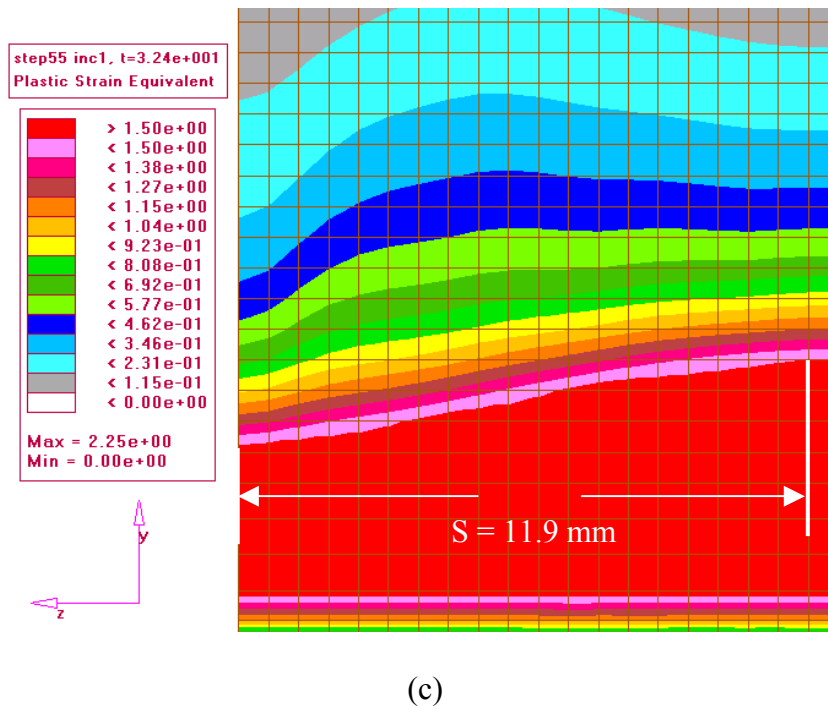
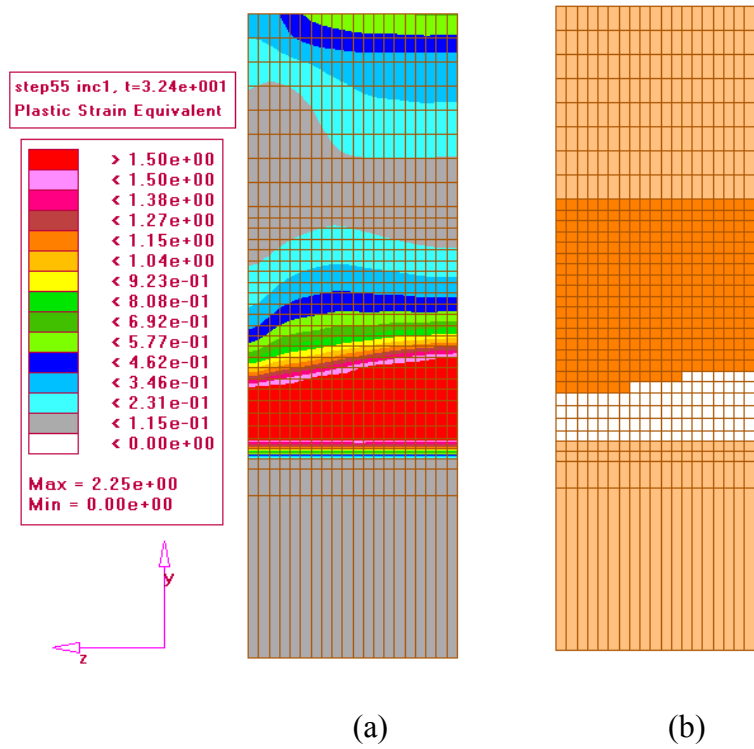


Figure 4.13: (a) Plastic Strain Contours, (b) Crack Propagation and (c) Close-up View of Plastic Strain Contours for Model With Curve 1 Material Properties Using Strain Energy Density as Removal Criterion ( $a/W = 0.4$ )

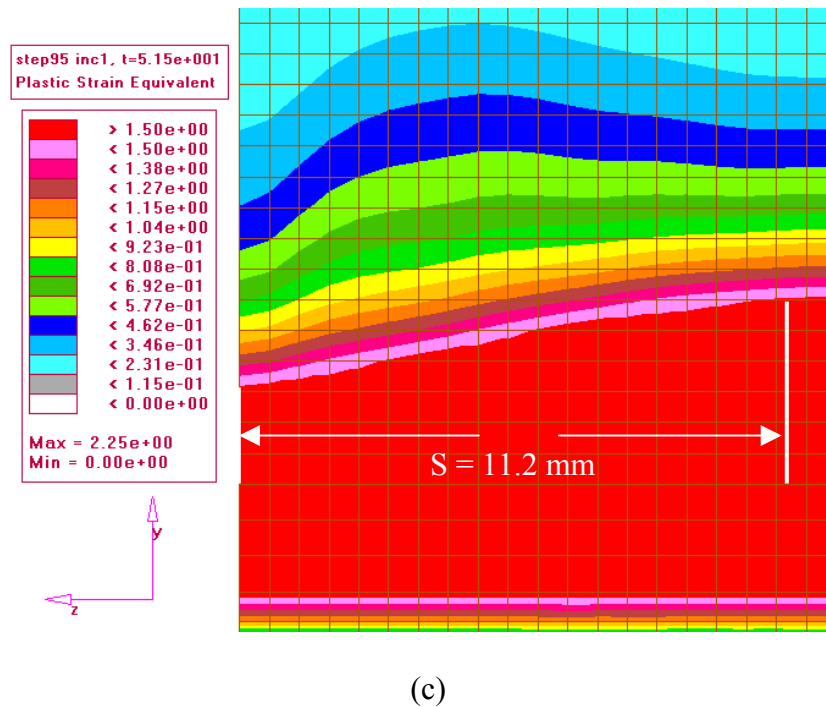
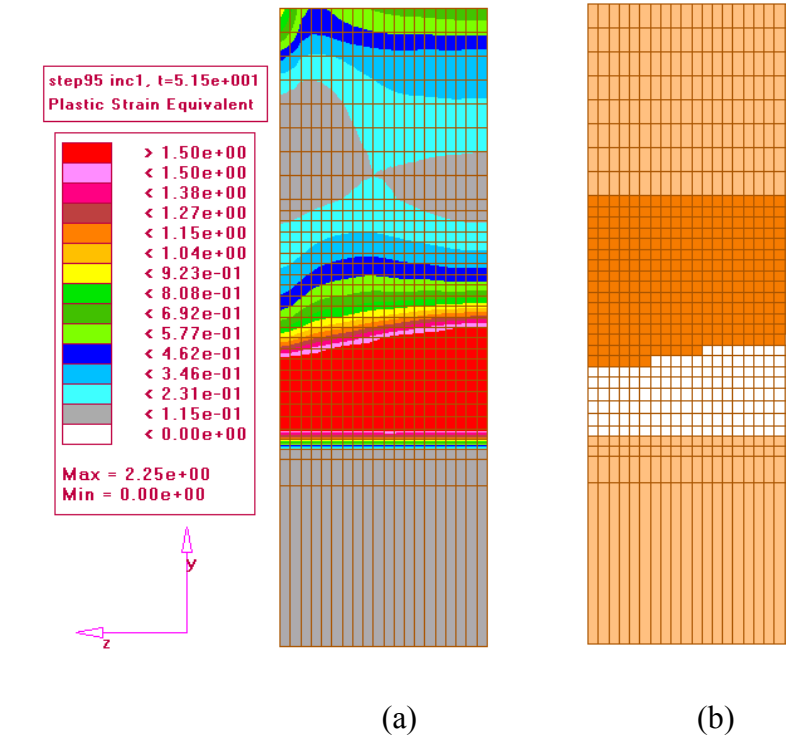


Figure 4.14: (a) Plastic Strain Contours, (b) Crack Propagation and (c) Close-up View of Plastic Strain Contours for Model With Curve 1 Material Properties Using Strain Energy Density as Removal Criterion ( $a/W = 0.43$ )

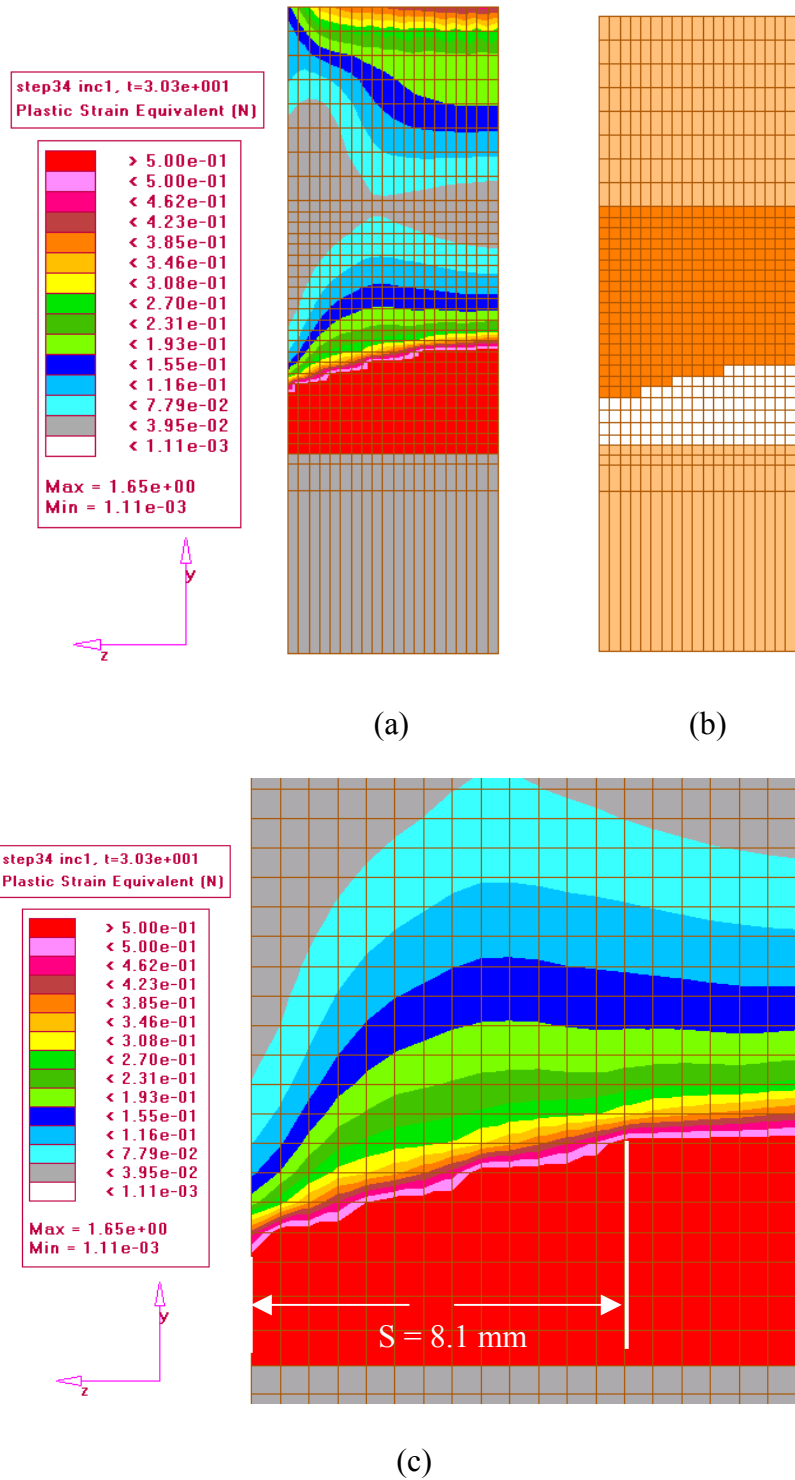


Figure 4.15: (a) Plastic Strain Contours, (b) Crack Propagation and (c) Close-up View of Plastic Strain Contours for Model With Curve 2 Material Properties Using Strain Energy Density as Removal Criterion ( $a/W = 0.4$ )

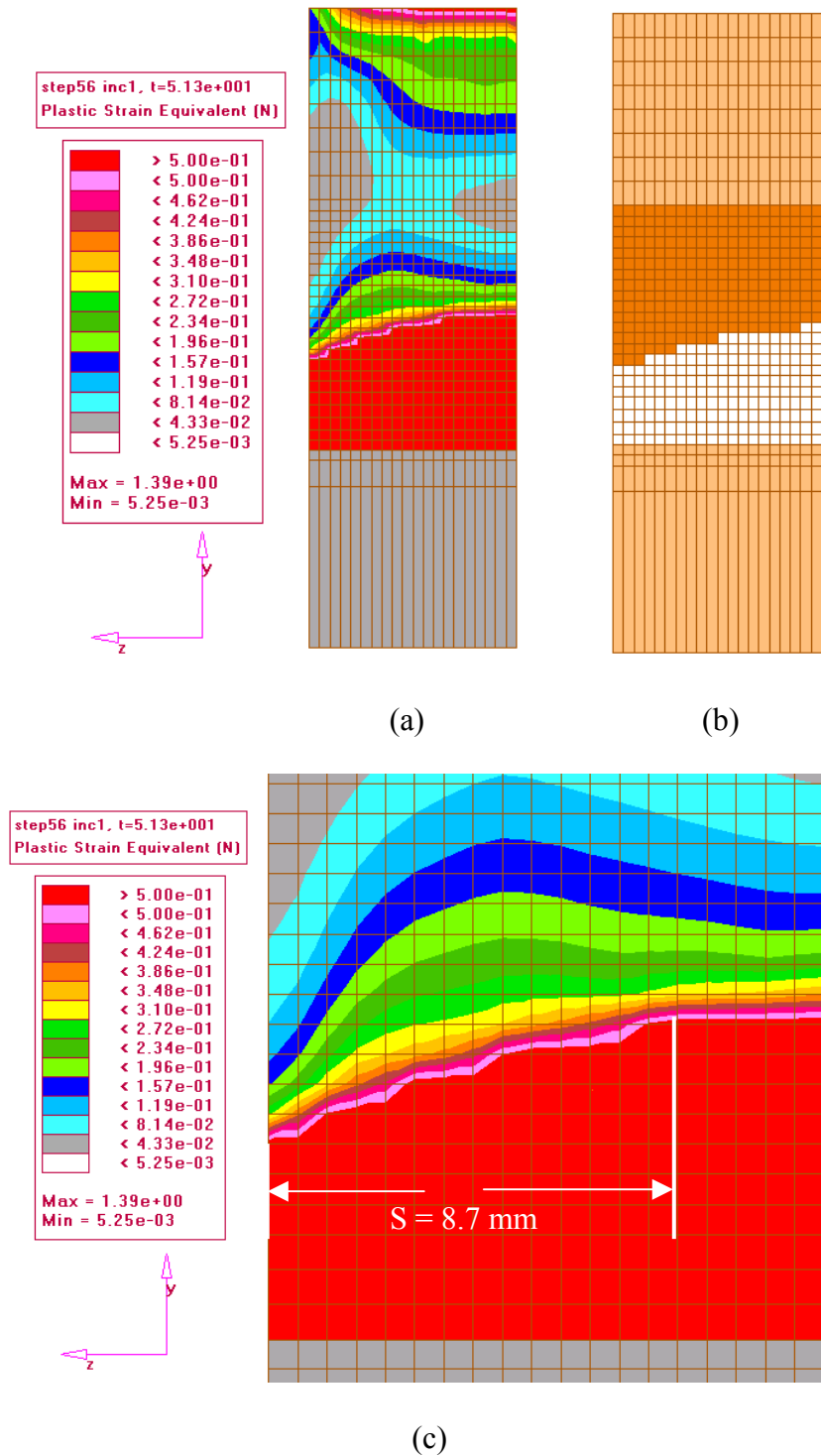


Figure 4.16: (a) Plastic Strain Contours, (b) Crack Propagation and (c) Close-up View of Plastic Strain Contours for Model With Curve 2 Material Properties Using Strain Energy Density as Removal Criterion ( $a/W = 0.45$ )

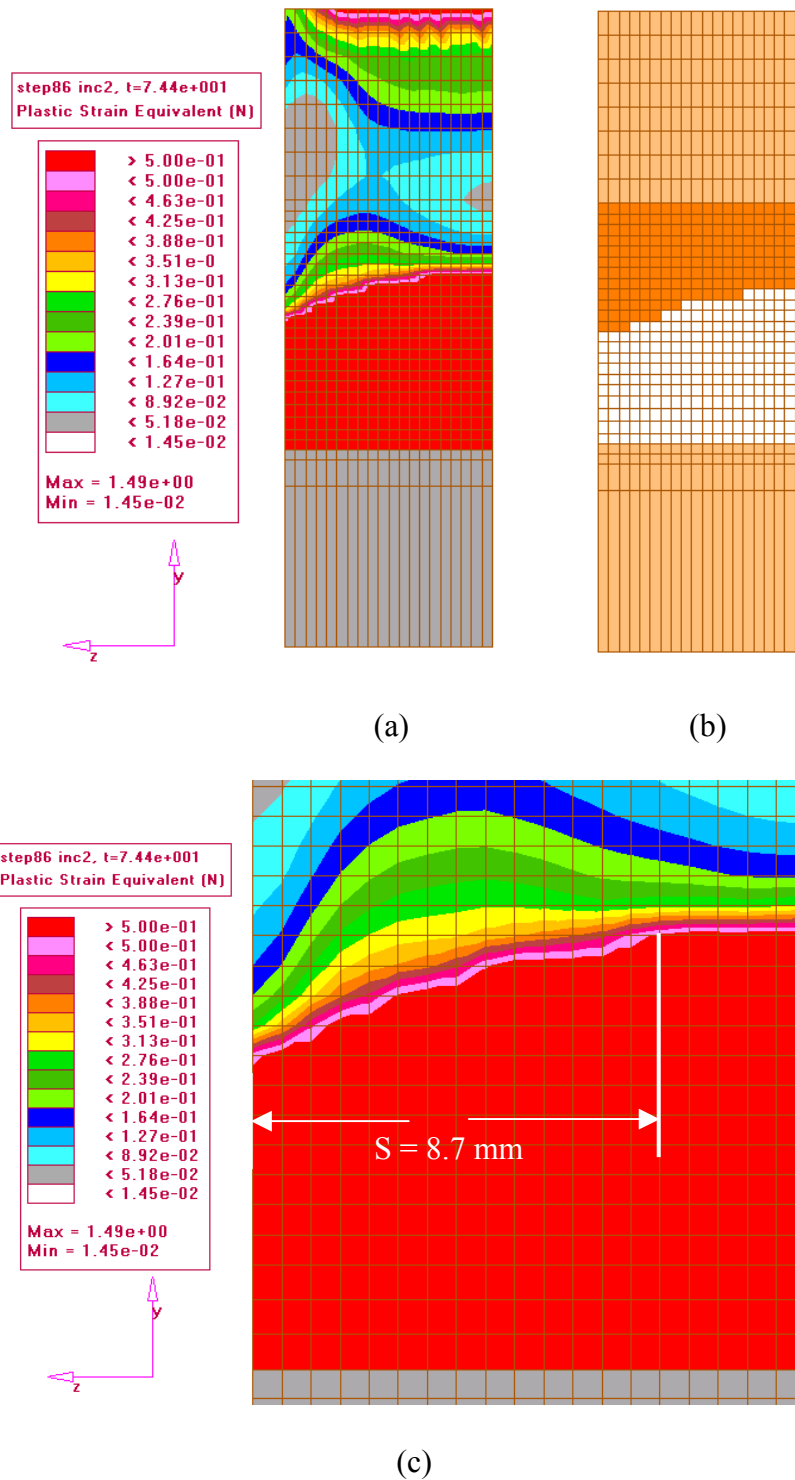


Figure 4.17: (a) Plastic Strain Contours, (b) Crack Propagation and (c) Close-up View of Plastic Strain Contours for Model With Curve 2 Material Properties Using Strain Energy Density as Removal Criterion ( $a/W = 0.5$ )

## **5. SUMMARY, CONCLUSIONS AND RECOMMENDATIONS**

### **5.1 Summary and Conclusions**

This study focused on the development of shear-lip in DT specimens under quasi-static loading rate. The objective of the study was to demonstrate the feasibility of a numerical simulation of shear-lips for a 25mm base metal DT specimen in three-point bend test. Three real stress-strain curves representing three different materials with varying degrees of plastic behaviour were considered. These material curves are designated as Curves 1, 2 and 3. Curve 1 represents the actual real-stress-strain curve of the 350WT steel material. On the other hand, Curve 2 represented the same curve, but with the fracture strain reduced to have that of Curve 1; while Curve 3 represents a similar curve as Curve 1, but with the yield stress reduced to half the Curve 1 value. Crack advance and element or node release was based on two possible criteria, namely (a) when the average strain in the crack tip elements that occupy a physical surface of 1.25 mm (0.050 inches) exceeds the strain at fracture on the supplied data; and (b) when the strain energy density in elements occupying a volume defined by 1.25 mm (0.050 inches) of free surface at the crack tip and 1.25 mm (0.050 inches) of material depth exceeds the strain energy density calculated from the supplied real stress-strain curves.

It was shown that the plastic strain contour patterns obtained from the finite element analyses could be used to estimate the shear-lip sizes. At any given crack size ( $a/W$  level), the shear-lip size is smallest for Curve 2 material and largest for Curve 3. This trend is reasonable as the Curve 2 material is the least plastic (100% strain to failure as opposed to 200% strain for Curves 1 and 3); and the Curve 3 material is the most plastic (has lower yield stress of 197MPa compared to 395MPa for Curves 1 and 2, and high failure strain of 200%). For a given material, the shear-lip size tends to reduce with increasing crack size. For instance, for the Curve 1 material, the shear-lip sizes for  $a/W = 0.4, 0.45$  and  $0.5$  are 10.95mm, 10.30mm and 9.70mm, respectively. The same trends of shear-lip sizes were observed, regardless of whether the plastic strain criterion or strain energy density criterion was used for crack advance. However, for any given material and crack size, the shear-lip size predicted based on the strain energy density criterion was greater than that predicted based on the plastic strain criterion.

## **5.2 Recommendations**

It is recommended that comparisons be made between the results obtained in this study and experimental studies being conducted at DRDC. Based on these comparisons, it might be necessary to refine the methodology presented. In this regard, issues that need consideration include investigation of the influence of mesh refinement and the use of strain energy density criterion that is obtained from tests in a triaxial state of stress. It is also recommended that the analysis be extended to specimens of different thickness (say 16mm and 12.5mm). Such studies could be used to correlate results from earlier DRDC studies [4] and hence lead to the use of the shear-lip size information as a material property.

## 6. REFERENCES

- [1] Koko, T.S., Gallant, B.K. and Tobin, S.M. "Investigation of Plastic Zone Development in Dynamic Tear Test Specimens." DREA, Contractor Report DREA-1999-095 July 1999.
- [2] Koko, T.S., Gallant, B.K. and Tobin, S.M. "Investigation of Plastic Zone Development in Dynamic Tear Test Specimens – Phase II." DREA, Contractor Report DREA-CR2000-115 September 2000.
- [3] Koko, T.S. and Gallant, B.K. "Investigation of Plastic Zone Development in Dynamic Tear Test Specimens – Phase III." Martec Report No.: TR-01-22, July 2001.
- [4] Matthews, J.R. "On the Relationship between Shear-lip, Shear Index and Energy in Dynamic Tear Specimens", Engineering Fracture Mechanics, Vol. 54, No. 1, pp. 11-23, 1996.
- [5] Degiorgi, V.G. and Matic, P. "A Computational Investigation of Local Material Strength and Toughness on Crack Growth", Engineering Fracture Mechanics, Vol. 37, No. 5, pp. 1039-1058, 1990.
- [6] Hibbitt, H.D. Karlsson, B.I. and Sorensen, E.P. ABAQUS User's Manual, 1990.
- [7] ANSYS Inc., ANSYS User's Online Help Manual, 2000.

DOCUMENT CONTROL DATA		
(Security classification of title, body of abstract and indexing annotation must be entered when the overall document is classified)		
1. ORIGINATOR (the name and address of the organization preparing the document.. Organizations for whom the document was prepared, e.g. Centre sponsoring a contractor's report, or tasking agency, are entered in section 8.)  Martec Limited 400-1888 Brunswick Street Halifax NS B3J 3J8	2. SECURITY CLASSIFICATION (overall security classification of the document including special warning terms if applicable).  UNCLASSIFIED	
3. TITLE (the complete document title as indicated on the title page. Its classification should be indicated by the appropriate abbreviation (S,C,R or U) in parentheses after the title).  Shear Lip/ Plastic Zone Finite Element Model Development		
4. AUTHORS (Last name, first name, middle initial. If military, show rank, e.g. Doe, Maj. John E.)  B.K. Gallant and T.S. Koko		
5. DATE OF PUBLICATION (month and year of publication of document)  October 2002	6a. NO. OF PAGES (total containing information Include Annexes, Appendices, etc).  53	6b. NO. OF REFS (total cited in document)  7
7. DESCRIPTIVE NOTES (the category of the document, e.g. technical report, technical note or memorandum. If appropriate, enter the type of report, e.g. interim, progress, summary, annual or final. Give the inclusive dates when a specific reporting period is covered).  CONTRACTOR REPORT		
8. SPONSORING ACTIVITY (the name of the department project office or laboratory sponsoring the research and development. Include address). Defence R&D Canada - Atlantic PO Box 1012 Dartmouth, NS, Canada B2Y 3Z7		
9a. PROJECT OR GRANT NO. (if appropriate, the applicable research and development project or grant number under which the document was written. Please specify whether project or grant).  Project 11 gn	9b. CONTRACT NO. (if appropriate, the applicable number under which the document was written).  W7707-8-6180/A	
10a ORIGINATOR'S DOCUMENT NUMBER (the official document number by which the document is identified by the originating activity. This number must be unique to this document.)	10b OTHER DOCUMENT NOS. (Any other numbers which may be assigned this document either by the originator or by the sponsor.)  DRDC Atlantic CR 2002-178	
11. DOCUMENT AVAILABILITY (any limitations on further dissemination of the document, other than those imposed by security classification) ( X ) Unlimited distribution ( ) Defence departments and defence contractors; further distribution only as approved ( ) Defence departments and Canadian defence contractors; further distribution only as approved ( ) Government departments and agencies; further distribution only as approved ( ) Defence departments; further distribution only as approved ( ) Other (please specify):		
12. DOCUMENT ANNOUNCEMENT (any limitation to the bibliographic announcement of this document. This will normally correspond to the Document Availability (11). However, where further distribution (beyond the audience specified in (11) is possible, a wider announcement audience may be selected).		

13. **ABSTRACT** (a brief and factual summary of the document. It may also appear elsewhere in the body of the document itself. It is highly desirable that the abstract of classified documents be unclassified. Each paragraph of the abstract shall begin with an indication of the security classification of the information in the paragraph (unless the document itself is unclassified) represented as (S), (C), (R), or (U). It is not necessary to include here abstracts in both official languages unless the text is bilingual).

This study focused on the development of shear-lip in DT specimens under quasi-static loading rate. The objective of the study was to demonstrate the feasibility of a numerical simulation of shear-lips for a 25mm base metal DT specimen in three-point bend test. Three real stress-real strain curves representing three different materials with varying degrees of plastic behaviour were considered. These material curves are designated as Curves 1, 2 and 3. Curve 1 represents the actual real-stress- real-strain curve of the 350WT steel material. On the other hand, Curve 2 represents the same curve, but with the fracture strain reduced to half that of Curve 1; while Curve 3 represents a similar curve as Curve 1, but with the yield stress reduced to half the Curve 1 value. Crack advance and element or node release was based on two possible criteria, namely (a) when the average strain in the crack tip elements that occupy a physical surface of 1.25 mm (0.050 inches) exceeds the strain at fracture on the supplied data; and (b) when the strain energy density in elements occupying a volume defined by 1.25 mm (0.050 inches) of free surface at the crack tip and 1.25 mm (0.050 inches) of material depth exceeds the strain energy density calculated from the supplied real stress real strain curves.

It was shown that the plastic strain contour patterns obtained from the finite element analyses could be used to estimate the shear-lip sizes. At any given crack size (a/W level), the shear-lip size is smallest for Curve 2 material and largest for Curve 3. This trend is reasonable as the Curve 2 material is the least plastic (100% strain to failure as opposed to 200% strain for Curves 1 and 3); and the Curve 3 material is the most plastic (has lower yield stress of 197MPa compared to 395MPa for Curves 1 and 2, and high failure strain of 200%). For a given material, the shear-lip size tends to reduce with increasing crack size. For instance, for the Curve 1 material, the shear-lip sizes for a/W = 0.4, 0.45 and 0.5 are 10.95mm, 10.30mm and 9.70mm, respectively. The same trends of shear-lip sizes were observed, regardless of whether the plastic strain criterion or strain energy density criterion was used for crack advance. However, for any given material and crack size, the shear-lip size predicted based on the strain energy density criterion was greater than that predicted based on the plastic strain criterion.

14. **KEYWORDS, DESCRIPTORS or IDENTIFIERS** (technically meaningful terms or short phrases that characterize a document and could be helpful in cataloguing the document. They should be selected so that no security classification is required. Identifiers, such as equipment model designation, trade name, military project code name, geographic location may also be included. If possible keywords should be selected from a published thesaurus. e.g. Thesaurus of Engineering and Scientific Terms (TEST) and that thesaurus-identified. If it not possible to select indexing terms which are Unclassified, the classification of each should be indicated as with the title).

shear lip  
plastic zone  
finite element  
dynamic tear specimen

## **Defence R&D Canada**

**Canada's leader in defence  
and national security R&D**

## **R & D pour la défense Canada**

**Chef de file au Canada en R & D  
pour la défense et la sécurité nationale**



**[www.drdc-rddc.gc.ca](http://www.drdc-rddc.gc.ca)**